Contract No:

This document was prepared in conjunction with work accomplished under Contract No. DE-AC09-08SR22470 with the U.S. Department of Energy (DOE) Office of Environmental Management (EM).

Disclaimer:

Corrosion of Steel During Long-Term Exposure to Evolving Cementitious Environments

B. J. Wiersma

April 30, 2021

SRNL-STI-2021-00187, Revision 0

DISCLAIMER

Printed in the United States of America

Prepared for
U.S. Department of Energy

SRNL-STI-2021-00187
Revision 0

Keywords: *Performance Assessment, Corrosion, Carbon Steel, Waste Tank*

Retention: *Varies*

Corrosion of Steel During Long-Term Exposure to Evolving Cementitious Environments

B. J. Wiersma

April 30, 2021

Prepared for the U.S. Department of Energy under
contract number DE-AC09-08SR22470.

REVIEWS AND APPROVALS

AUTHOR:

_____

B. J. Wiersma, Applied Materials Research Date
Savannah River National Laboratory

TECHNICAL REVIEW:

_____

X-K. Zhu, Applied Materials Research, Reviewed per E7 2.60 Date
Savannah River National Laboratory

_____

G. P. Flach, Closure and Disposal Assessment Date
Savannah River Remediation

APPROVAL:

_____

S. D. Fink, Director, Chemical Processing Technology Date
Savannah River National Laboratory

_____

K. H. Rosenberger, Manager, Closure and Disposal Assessment Date
Savannah River Remediation

ACKNOWLEDGEMENTS

I would like to acknowledge the beneficial discussions that were held with G. P. Flach, M. H. Layton and X-K. Zhu who provided constructive feedback on the model approach and checked all the detailed calculations. This paper was written while teleworking from home during the year of the pandemic. I would also like to thank my wife and family who allowed me to concentrate and complete the report.

EXECUTIVE SUMMARY

SRS is proceeding with closure of the H-Area Tank Farm (HTF) and F-Area Tank Farm (FTF). Closure consists of removing the bulk waste, heel removal, and filling the tank with tailored grout formulations. The long-term performance of the concrete and steel materials of construction and the closure grout is an important consideration for Performance Assessment (PA) of closed tanks in FTF and HTF.

Over PA timeframes of hundreds, thousands, to tens of thousands of years, the chemical and physical properties of the concrete and steel materials will slowly degrade due to environmental exposure and material aging. In the interim these materials will provide a barrier to the leaching of radionuclides into the soil. Savannah River Remediation (SRR) is updating relevant portions of these analysis inputs to support an imminent revision to the HTF PA and a future update to the FTF PA. This analysis provides an update to the previous PA inputs for steel corrosion.

The Central Scenario for the PA analysis includes three postulated modeling cases: 1) Realistic Case, 2) Compliance Case, and 3) Pessimistic Case. This analysis also included a Fast Flow Path Case. This latter case considered the circumstance where the initial condition of the concrete was a completely degraded state and that grout shrinkage exposed the steel to the soil environment immediately. In effect, the steel was unprotected by the concrete and grout. The cases have various degrees of conservatism considered. Chemical, physical and tank configuration parameters were investigated to understand their effects on the predicted time to release of the contaminants. The assessment reviewed the initial tank and steel configuration, service life degradation of the steel, and potential corrosion mechanisms associated with degradation of the concrete materials.

The key observations and results are:

- The progressive degradation model for the steel provides a new approach for the steel corrosion PA input.
- Corrosion mechanism inputs were the same or slightly revised from the previous analysis inputs.
- There is a strong link between the degradation of the concrete and steel corrosion rate. Likewise, there is a link between the steel degradation and the concrete degradation rate. The steel liner progression model discussed herein coupled the two degradation models to provide SRR with an estimate for the release time of radioactive contaminants to the environment.
- Table ES-1 for the Saturated Zone and Table ES-2 for the Vadose Zone summarize the range of failure times across tank components for the various PA modeling cases as a function of waste tank type. Tank components include the floor, wall, and roof portions of the primary and secondary steel liners. Saturated and Vadose Zone values apply to tank components below and above the water table, respectively.
- Table ES-3 shows the failure times for the cooling coils that are embedded in grout upon tanks closure inside the Type I, II, and III/IIIA tanks. The failure time is shown as a

function of the assumed case. Given that the pipe is the same size in all the tanks, the failure time is independent of the tank type.

- The models make simplifying and generally conservative assumptions regarding the corrosion response to a change in the environment and the effects of cracks on the corrosion rate. These assumptions could be refined further to reduce uncertainty in the predicted times.

Table ES-1. Summary of Failure Times (years) for the Saturated Zone for the Scenario Cases by Tank Type

	Saturated Zone			
Tank Type	Realistic Case (years)	Compliance Case (years)	Pessimistic Case (years)	Fast Flow Path Case (years)
I	3929-6250	3929-6250	625-3941	13-65
II	6250-10938	6250-10938	704-6250	14-65
III/IIIA	4688-10938	4688-10938	625-6250	13-59
IV	2495-5469	2495-5469	852-2477	20-42

Table ES-2. Summary of Failure Times (years) for the Vadose Zone for the Scenario Cases by Tank Type

	Vadose Zone			
Tank Type	Realistic Case (years)	Compliance Case (years)	Pessimistic Case (years)	Fast Flow Path Case (years)
I	4008-6250	2960-6250	625-850	123-502
II	6250-10938	4280-8719	704-1136	123-502
III/IIIA	4688-10938	3860-7751	625-1078	92-441
IV	2569-5469	1082-1127	263-367	181-226

Table ES-3. Summary of Cooling Coil Failure Times (years) for Each Case

Case	**Failure Time (years)**
Realistic Case	1925
Compliance Case	350
Pessimistic Case	350
Fast Flow Path Case	38

TABLE OF CONTENTS

LIST OF TABLES

LIST OF FIGURES

LIST OF ABBREVIATIONS

ACI	American Concrete Institute
ASTM	ASTM International, formerly known as the American Society for Testing and Materials
COA	Crack Opening Area
FTF	F-Area Tank Farm
HLW	High Level Waste
HTF	H-Area Tank Farm
mil	1 mil = 0.001 inches
mpy	mils/year
NBS	National Bureau of Standards
PA	Performance Assessment
rebar	reinforcing bar in concrete
SCC	Stress Corrosion Cracking
SDW	Simulated Dilute Water
SRNL	Savannah River National Laboratory
SRR	Savannah River Remediation
SRS	Savannah River Site
YMP	Yucca Mountain Project

1.0 Introduction

Liquid radioactive and chemical waste has been stored in large (i.e., approximately 1 million gallon), underground tanks at the Savannah River Site (SRS) for nearly 70 years. The tanks were constructed of carbon steel materials and were encased in concrete vaults to provide structural stability for the below-grade tanks. SRS is proceeding with closure of waste tanks within the H-Area Tank Farm (HTF) and F-Area Tank Farm (FTF). Closure consists of removing the bulk waste, heel removal, and filling the tank with tailored grout formulations.

The long-term performance of the concrete and steel materials of construction and the closure grout is an important consideration for Performance Assessment (PA) of closed tanks in FTF and HTF. Over PA timeframes of hundreds, thousands, to tens of thousands of years, the chemical and physical properties of the concrete and steel materials will slowly degrade due to environmental exposure and material aging. In the interim these materials will provide a barrier to the leaching of radionuclides into the soil. The current FTF and HTF PAs [1], [2] are based on multiple studies that consider the chemical and/or physical degradation of cementitious materials, either directly or indirectly [3], [4], [5], [6], [7]. Savannah River Remediation (SRR) is updating relevant portions of these studies to support an imminent revision to the HTF PA and a future update to the FTF PA.

This investigation focuses on the degradation of the steel materials due to corrosion [8], [9]. Corrosion initiation and propagation is coupled to the quality of the cementitious material that contacts the steel. For concrete and grout, the high pH environment creates a passivated surface oxide on the steel that minimizes corrosion of steel. Unless this passive oxide is disrupted, the steel will corrode at a very low, general rate. However, if the concrete degrades due to chemical or physical changes, aggressive species such as chloride, oxygen, or carbon dioxide will migrate to the steel and initiate and propagate corrosion. SRR has updated the analysis for cementitious material degradation in coordination with this study [10]. SRNL was requested to concurrently assess how the changes to the analysis will influence corrosion of the steel components. This analysis will provide an update to the previous PA inputs for steel corrosion [6], [7].

The Central Scenario for the PA analysis includes three postulated cases: 1) Realistic Case, 2) Compliance Case, and 3) Pessimistic Case. This analysis also included a Fast Flow Path Case. This latter case considered the circumstance where the concrete was completely degraded initially, and grout shrinkage exposed the steel to the soil environment immediately. In effect, the steel was unprotected by the concrete and grout. The cases have various degrees of conservatism considered. Chemical, physical and tank configuration parameters were investigated to understand their effects on the predicted time to release of the contaminants. The assessment reviewed the initial tank and steel configuration, service life degradation of the steel,

and potential corrosion mechanisms associated with degradation of the concrete and grout materials.

Limiting life calculations were made that considered both the corrosion of the steel and the influence of concrete degradation on the corrosion of the steel. The results illustrate how steel degradation progresses with time (i.e., which mechanisms are significant) and which configuration and chemical properties are significant.

2.0 Steel Tank and Concrete Vault Descriptions

2.1 Type I Waste Tanks

The primary and secondary walls for the Type I waste tanks were constructed of ASTM Type A285-50T, Grade B Steel, with the nominal composition shown in Table 2-1 [11].

Table 2-1. Non-Iron Composition of ASTM A285-50T Grade B Steel

	Composition wt.%			
For plates ≤ 0.75 inch thick	**C max**	**Mn max**	**P max**	**S max**
	0.2*	**0.8**	**0.035**	**0.04**

* C = 0.22% for plate thicknesses between 0.75 and 2 inches

Type I tanks (shown in Figure 2-1) have a nominal capacity of 750,000 gallons, are 75 feet in diameter, and 24.5 feet high. The primary tanks are a closed cylindrical tank with flat top and bottom constructed from 0.5-inch thick steel plate. The top and bottom are joined to the cylindrical sidewall by curved knuckle plates. The tanks are constructed with a top weld to the top of the tank, middle welds between plates, and bottom welds to the bottom of the plate. A 5-foot high steel pan provides partial secondary containment for the tanks and a concrete vault encompassing the primary tank and the steel pan provides additional containment. The Type I tanks are not stress relieved.

The concrete vault provides a barrier between the soil and the tank steel. The Type I tanks are unusual in that they are completely buried in the soil, approximately 9 feet below grade. The concrete was placed according to the DuPont Site Specification 3557 of record at the time the tanks were built [12]. A review of the requirements indicated a good quality concrete material was produced if the specification was followed. That is, the concrete would have low air content and a relatively low water/cement ratio, qualities that would restrict the permeability of gases into the concrete.

The tank and pan are set on a 30-inch thick base slab and are enclosed by a cylindrical 22-inch thick reinforced concrete wall and a flat 22-inch thick concrete roof. There are twelve 2-foot

diameter concrete columns within the primary tank to support the roof. Each column has a flared capital and is encased in 0.5-inch thick A285 carbon steel plate.

The concrete reinforcing bar (rebar) material was ASTM A615 Grade 40 [12]. According to ASTM A510 [13], there are several grades of carbon steel that would meet the chemical and mechanical property criteria cited in ASTM A615 [14]. The decision on which grade of carbon steel was used for rebar would have depended upon availability. Based on previous corrosion tests with different grades of carbon steel, no significant difference would be anticipated in their corrosion behavior. Drawings of the concrete vault indicated that the rebar size was typically between 0.75 to 0.875 inches in diameter and spaced between 6 to 7.5 inches apart [15].

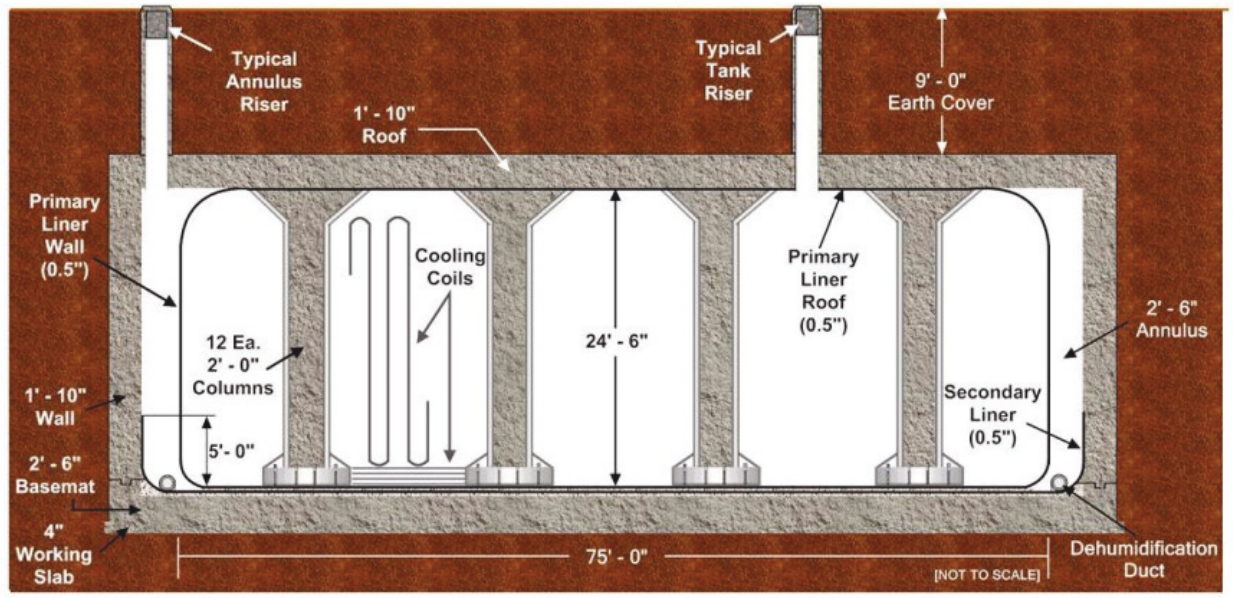

Figure 2-1. Design of Type I Waste Tank **[1]**

2.2 Type II Waste Tanks

Type II tanks were also constructed using A285 Grade B carbon steel. The composition for the steel in Type II tanks is the same as for Type I tanks and is detailed in Table 2-1 [11]. Type II tanks have a diameter of 85 feet and are 27 feet high with a capacity of 1,030,000 gallons (Figure 2-2).

The primary tank within a Type II tank is annular in shape with a central concrete roof support that rests on the bottom slab of the tank. The outer cylinder of the tank is joined to the top and bottom plates by curved knuckle plates. The nominal thicknesses of the cylinder walls are listed in Table 2-2.

Table 2-2. Type II Tank Wall Thickness

Plate	Thickness (in.)
Top and Bottom	1/2
Upper Knuckle	9/16
Wall	5/8
Lower Knuckle	7/8

A five-foot high carbon steel pan provides secondary containment for the Type II tanks and forms an annular space where leaking waste may collect.

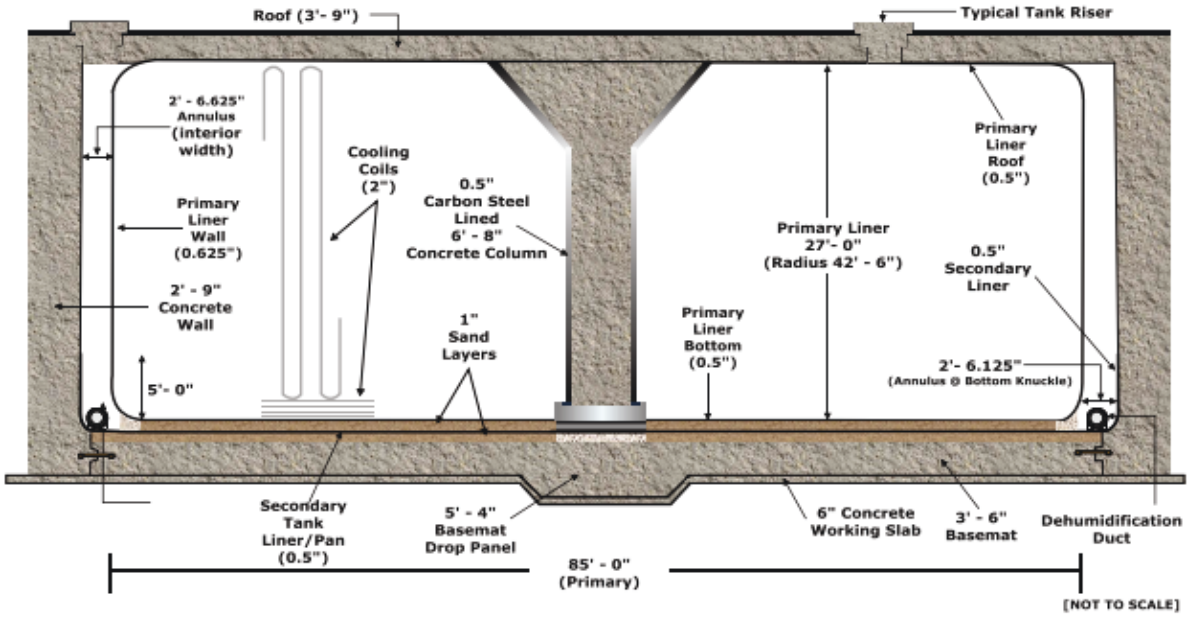

Figure 2-2. Design of Type II Waste Tank [1]

The concrete vault for the Type II tanks is surrounded on three sides by soil, while the roof is at grade-level. The concrete was placed according to the DuPont Site Specification 3557 of record at the time the tanks were built [12]. A review of the requirements indicated a good quality concrete material was produced if the specification was followed. That is, the concrete would have low air content and a relatively low water/cement ratio, qualities that would restrict the permeability of gases into the concrete.

The tank and secondary pan assembly are set on a concrete foundation slab that is 42 inches thick. The primary is enclosed by a cylindrical reinforced concrete wall that is 33 inches thick and a flat concrete roof that is 45 inches thick. The roof is supported by the walls and a central concrete column nestled within the inner cylinder of the vessel.

The rebar material was ASTM A615 Grade 40 [12]. According to ASTM A510 [13], there are several grades of carbon steel that would meet the chemical and mechanical property criteria cited in ASTM A615 [14]. The decision on which grade of carbon steel was used for rebar would have depended upon availability. Based on previous corrosion tests with different grades of carbon steel, no significant difference would be anticipated in their corrosion behavior. Drawings of the concrete vault indicated that the rebar size was typically between 1.12 to 1.41 inch in diameter and spaced between 5 and 10 inches apart [16].

2.3 Type III/IIIA Waste Tanks

The most recently constructed double shell tanks are designated as Type III/IIIA tanks. Twenty-seven Type III/IIIA tanks were constructed between 1967-1981 in both F and H areas. Figure 2-3 shows a cross-sectional drawing of a Type III/IIIA tank. Each tank is 85 feet in diameter and 33 feet high with a capacity of 1,300,000 gallons [17]. Type III tanks have a toroidal shape similar to the Type II design. Each primary vessel is made of two concentric cylinders joined to washer-shaped top and bottom plates by curved knuckle plates. The plates used to form the primary were of varying thicknesses and are summarized in Table 2-4. The secondary vessel is 90 feet in diameter and 33 feet high (i.e., the full height of the primary tank) and is made of 0.375-inch thick steel.

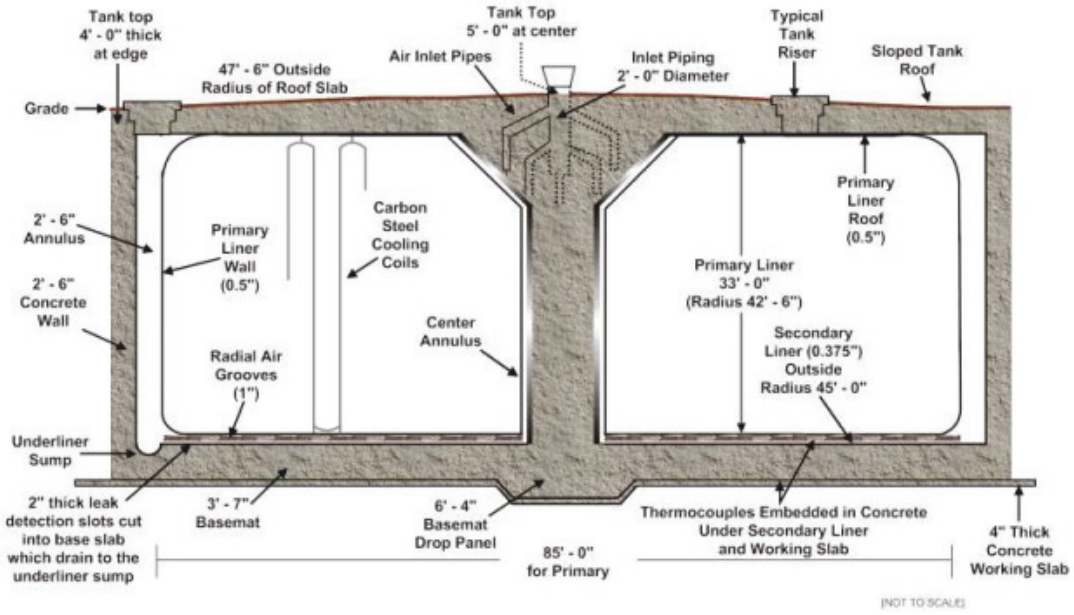

Figure 2-3. Design of Type III/IIIA Waste Tank [1]

The primary walls for the Type III waste tanks were made of ASTM Type A516 (A516) carbon steel [18], while for the Type IIIA waste tanks ASTM Type A537 (A537) carbon steel [19] was utilized. The steel for the secondary liner was A516. The nominal composition for each steel is shown in Table 2-3.

Table 2-3. Non-iron Composition of ASTM A516 and A537 Carbon Steel

Steel Specification	C_{max} (wt.%)	Mn (wt.%)	P_{max} (wt.%)	S_{max} (wt.%)
A516	0.27	0.6-0.9	0.035	0.035
A537	0.24	0.7-1.35	0.035	0.035

Table 2-4. Steel Plate Thickness in Type III/IIIA Waste Tanks

Plate	Thickness, in.
Top and Bottom	1/2
Upper Knuckle	1/2
Outer cylinder wall	
Upper band	1/2
Middle band	5/8
Lower band	3/4
Inner cylinder wall	
Upper band	1/2
Lower band	5/8
Lower knuckle	
Outer cylinder	7/8 (Tanks 25-28 and 33-51) 1 (Tanks 29-32)
Inner cylinder	5/8

The concrete vault for the Type III/IIIA tanks is also surrounded on three sides by soil, while the roof is at grade-level. The concrete was placed according to the DuPont Site Specification 3557 of record at the time the tanks were built [12]. A review of the requirements indicated a good quality concrete material was produced if the specification was followed. That is, the concrete would have low air content and a relatively low water/cement ratio, qualities that would restrict the permeability of gases into the concrete.

The primary tank rests on a 6-inch bed of refractory concrete. Beneath the refractory is a minimum 42-inch thick concrete foundation slab. The cylindrical walls of the secondary are enclosed by a 30-inch thick reinforced concrete wall and a 48-inch thick flat reinforced concrete roof. Typically, there is three inches of cover above the reinforcement steel. A central concrete column fits within the inner cylinder of the vessel.

The rebar material was either ASTM A615 Grade 40 or Grade 60 [12]. Type III tanks built before 1972 utilized Grade 40, while the Type IIIA tanks utilized Grade 60. Figure 2-4 shows the rebar utilized for a Type III/IIIA waste tank. The secondary wall and the transfer lines that go into the tank are also visible. The difference between the two tank configurations is the

minimum required tensile strength (40 vs. 60 ksi). According to ASTM A510 [13], there are several grades of carbon steel that would meet the chemical and mechanical property criteria cited in ASTM A615 [14]. The decision on which grade of carbon steel was used for rebar would have depended upon availability. Based on previous corrosion tests with different grades of carbon steel, no significant difference would be anticipated in their corrosion behavior. Drawings of the concrete vault indicated that the rebar size was typically between 1.12 to 1.41 inches in diameter and spaced between 4 to 16 inches apart [20].

Figure 2-4. Rebar for a Type IIIA Waste Tank [2]

2.4 Type IV Waste Tanks

Tank 17F-20F and 21H-24H are single-walled, uncooled tanks and are designated as Type IV tanks. Tanks 17F-20F were constructed in 1958, while Tanks 21H-24H were constructed between 1959-61 [17]. Each tank is 85 feet in diameter and 34 feet high and has a capacity of 1,300,000 gallons. The tanks are essentially a steel lined, pre-stressed concrete vertical cylinder with a domed roof (see Figure 2-5). The carbon steel plates used to line the cylindrical walls and the tank bottom were 3/8 inch thick. The knuckle plates at the junction of the bottom and side wall are 7/16 inch thick.

The FTF Type IV tanks (17-20) were constructed of A285 carbon steel (see Table 2-1), while the HTF Type IV tanks (21-24) were constructed of ASTM A212 carbon steel . The A212 grade was a predecessor to ASTM A516 [21], thus the composition is similar to that shown in Table 2-3.

The concrete vault is buried in the soil with the roof rising above the surrounding grade level. The concrete was built-up around the steel vessel by the "shotcrete" technique, a pneumatic method of application in which a thick, semi-fluid mixture is blown through a nozzle [17]. The concrete dome roof, sidewall, and floor are all approximately 7 inches thick.

The wall was pre-stressed by embedding girths of steel under tension in the outer layers of the concrete wall. The rebar diameter was typically between 0.5 to 0.75 inches and the bars were 4 to 6 inches apart for the floor and sidewall; for the roof the spacing was typically 12 inches [22].

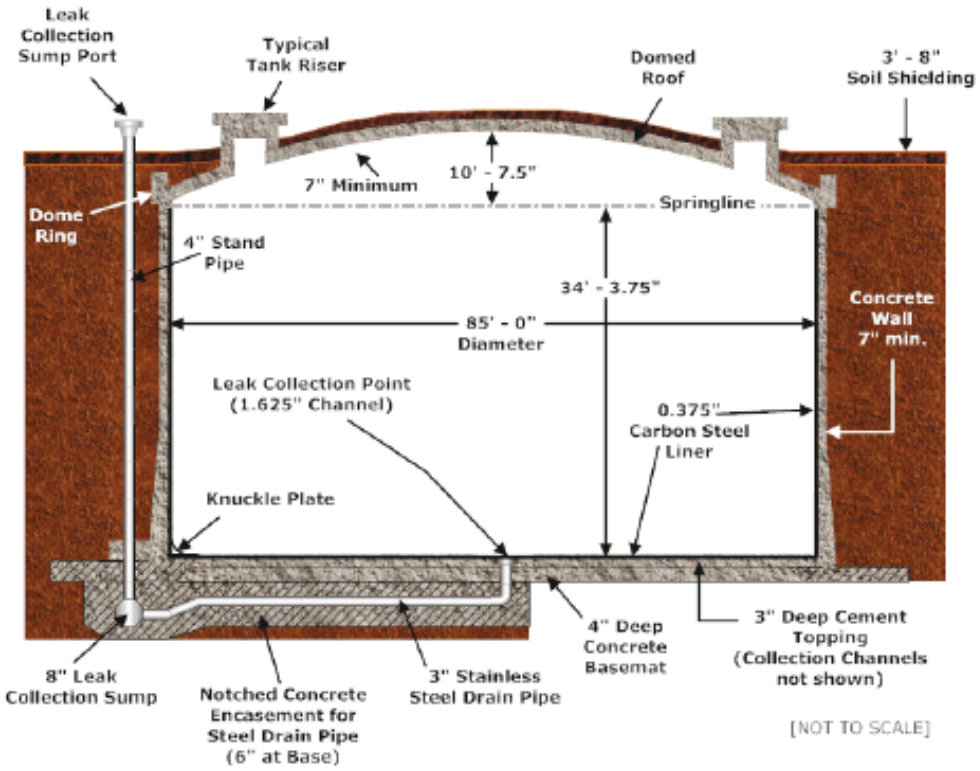

Figure 2-5. Design of Type IV Waste Tank [1]

2.5 In-Service Degradation of Steel and Concrete

2.5.1 Steel

Routine visual and ultrasonic inspections of the primary and secondary steel have been made through the service life of the tanks. Between 1972-1985, wall thickness ultrasonic measurements for general corrosion were made on all the tanks [23]. All measurements indicated that the average wall thickness remained at values greater than nominal for a given plate even after up to 30 years of service life. An example, of data from an inspection of the Tank 15 primary tank is shown in Figure 2-6 [24]. Tank 15 is a Type II waste tank.

Since 1994, ultrasonic measurements for general, pitting and stress corrosion cracking have been performed [25]. The measurements have been made on Type I, II, III/IIIA waste tanks. All measurements have indicated that both the secondary and primary steel have average wall thicknesses that remain at values greater than nominal for a given plate after up to 60 years of service life [26]. This also includes tanks that have been exposed to oxalic acid for the purpose of heel removal [27], [28]. An example of data from an inspection of the primary wall of Tank 25, a Type IIIA tank is shown in Figure 2-7 [29]. An example of data from the inspection of the secondary wall from Tank 40, a Type IIIA tank is shown in Table 2-5. These latest inspections have occasionally shown that there are local areas where the steel is slightly less than nominal. However, these areas are related to construction, not service, and tend to be small and isolated. The measurements show that the wall thickness has not changed significantly in the last 10 years [30].

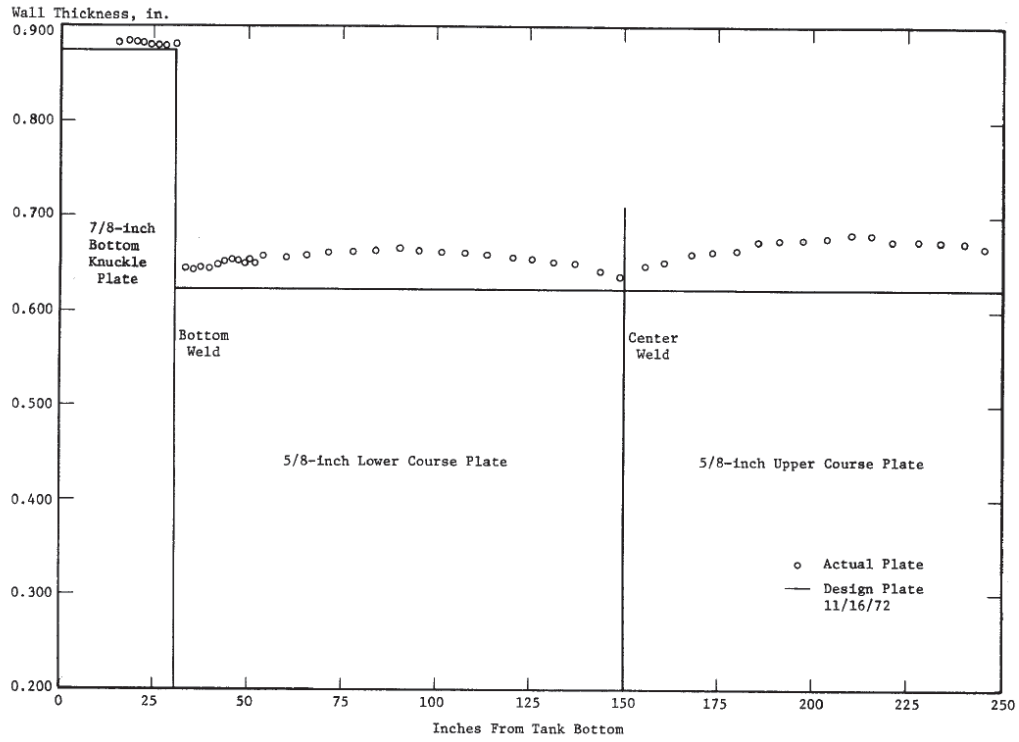

Figure 2-6. Wall Thickness Measurements from Ultrasonic Inspection of Tank 15 [24].

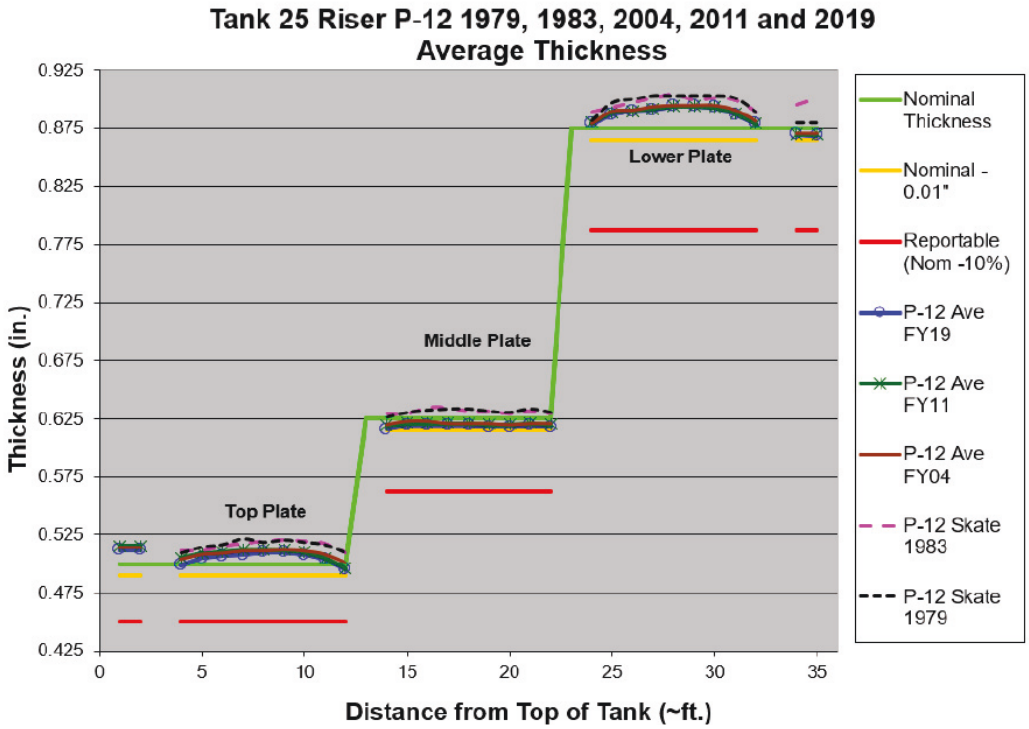

Figure 2-7. Tank 25 Ultrasonic Measurements for Average Wall Thickness from 1979-2019.

The ultrasonic inspections have also not revealed any significant service induced pitting corrosion. The deepest pits observed in a structure are on the order of 7% of the wall thickness and are not in clusters that would produce an area of thinning [31]. It is believed, based on the morphology of these pits, that many of these pits were pre-service.

A service life estimation for the tanks was performed to project the anticipated end-of-life [32]. The conclusion from the report was that significant degradation of the tanks due to general corrosion or pitting is not be anticipated if the waste environment remains within the parameters of the waste chemistry corrosion control program [33]. The effectiveness of the corrosion control program has been demonstrated by the present ultrasonic inspection program [25]. Thus, if operations continue to execute the corrosion control program prior to heel removal and the tanks are closed and filled with grout within a reasonable time (e.g., 50 years), the nominal thickness for the primary and secondary steel is a reasonable initial condition assumption for this analysis.

Table 2-5. Tank 40 Ultrasonic Measurements of Secondary Wall and Annulus Floor 2006 and 2016.

Tank 40 Plate / 12 inch segment	Nominal	Nominal - 0.01" *	P12 Ave, FY16	P12Ave, FY06
Plate 1 / 1	0.375	0.365	0.367	0.368
2	0.375	0.365	0.366	0.368
3	0.375	0.365	0.367	0.369
Plate 2 / 1	0.375	0.365	0.366	0.367
2	0.375	0.365	0.365	0.367
3	0.375	0.365	0.366	0.368
Plate 3 / 1	0.375	0.365	0.387	0.388
2	0.375	0.365	0.386	0.387
3	0.375	0.365	0.385	0.385
Plate 4 / 1	0.375	0.365	0.385	0.387
2	0.375	0.365	0.385	0.387
3	0.375	0.365	0.385	0.386
Secondary Floor	0.375	0.365	0.377	0.375

* Construction minimum thickness

The third corrosion mechanism of concern is stress corrosion cracking (SCC). This mechanism occurs due to the simultaneous presence of a susceptible material, a tensile stress, and an aggressive environment. This mechanism has led to leakage from several of the Type I and II waste tanks [17]. These tanks were not post weld heat treated during fabrication. Thus, residual stresses near welds, weld repairs, and weld attachments remained when the tanks were placed in service [34]. These tanks were also placed in service prior to the development and enforcement of the current corrosion control program [33]. Thus, partial and through-wall cracks have formed and have limited the usage of these tanks. A summary of the cracks and their location may be found in reference [35].

The most direct way for waste to leak through the steel tank liner would be through existing cracks in the tanks. Therefore, calculating the crack opening area (COA) in the tanks is important to determining the significance of leakage from tanks in the H-Tank Farm. The fracture mechanics methodology for the calculation used in the F-Tank Farm life assessment has been adopted to estimate the COA in the H-Tank Farm.

Separate calculations were performed to estimate crack areas for axial and circumferential cracks in the tanks. The derivations of the model equations for axial and circumferential COA are detailed in [6]. The model equation for axial COA is:

$$A = \frac{\sigma_y}{E} 2\pi Rt\left(\lambda^2 + 0.625\lambda^4\right) \text{ where } \lambda = \frac{a}{\sqrt{Rt}} \qquad \text{Equation 1}$$

where:

A	=	Crack Opening Area (in^2),
E	=	Young's Modulus (psi),
σ_y	=	Yield Stress (psi),
R	=	Radius of the Inner Surface (in),
t	=	Thickness (in),
λ	=	Dimensionless Crack Length, and
a	=	Crack Length (in).

The model equation for the COA in a circumferential flaw is:

$$A = \frac{4\sigma_y \pi (2t)^2}{E}\left(1 - \sqrt{\sqrt{1+\alpha^4} - \alpha^2}\right) \text{ where } \alpha = \frac{a}{2t} \qquad \text{Equation 2}$$

where:

α	=	Dimensionless Crack Length.

The parameters for the calculations of COA are shown in Table 2-6. The reference length for cracks in the tanks is 6 inches as estimated in previous reports on the tanks [36]. The crack length used is based on conservative estimates. It should be noted that unique cracks up to 18 inches long have been identified in the upper regions of at least 4 tanks since the original issue of this report [35]. However, the 6 inch or less crack that is perpendicular to the weld remains the most prevalent and therefore will continue to be used for this analysis. The mechanical properties of the tank steel are assumed not to significantly change from the base metal used for tank construction. The tank radius and thicknesses were calculated for the outer-most wall of the primary waste tank.

The COA model results are shown in Table 2-7. The calculations give the area for an individual crack in a Type I and Type II waste tank.

Table 2-6. Parameters for the axial and circumferential COA models

a	6	in.
E	30,000,000	psi
Yield Stress (ASTM A285)	27,000	psi
R (Type I)	450	in.
R (Type II)	510	in.
t (Type I)	0.5	in.
t (Type II)	0.625	in.

Table 2-7. Results for the COA calculations on an individual crack

Tank Type	Wall Thickness (in)	Axial COA (in^2)	Circumferential COA (in^2)
Type I	0.5	0.022	0.010
Type II	0.625	0.025	0.015

A conservative estimate of the total crack area for each waste tank could be obtained by multiplying the number of cracks in a tank by the circumferential COA since most cracks from stress corrosion cracking are perpendicular to the axial welds. The total estimated COA is calculated in Table 2-8.

For Type I tanks, the COA is always below 0.5 in^2. The COA for Type II tanks, except for Tank 13, was typically larger than for the Type I tanks. The COA for Tank 16 is 5.25 in^2 and is much larger than the other Type II tanks. However, even the large for Tank 16 is negligible compared to the total area of the waste tank. Therefore, the COA for the tanks is not considered in the analysis.

Table 2-8. Total Estimated COA for Type I and Type II Tanks

Tank Number	Tank Type	Number of Leaksites	Circumferential COA (in^2)
1	I	1	0.01
4	I	4	0.04
5	I	44	0.44
6	I	11	0.11
9	I	4	0.04
10	I	1	0.01
11	I	2	0.02
12	I	5	0.05
13	II	2	0.03
14	II	50	0.75
15	II	20	0.30
16	II	350	5.25

2.5.2 Concrete

A typical concrete vault for a Type III/IIIA tank is shown in Figure 2-8. A condition assessment of the accessible portions of the tank vault concrete was performed in 1993 [37]. For the Type I and II tanks and the interior of the concrete vault sidewall and roof, photographs of the concrete surface were reviewed. For the III/IIIA tanks, walkdowns of the exterior surface of the concrete roof were performed. Finally, for the Type IV tanks, photographs of the interior roof concrete surface were reviewed.

All interior surfaces of the Type I, II, and IV tanks were in excellent condition. No evidence of significant cracking, spallation, or rust stains were observed. Some indications of decalcification were evident, particularly on the dome of the Type IV tanks; however, the degradation was minor. The exterior surface of the roof for the Type III/IIIA tanks was also in excellent condition. There was no evidence of cracking, spalling or rust stains on the surface. There was some mechanical damage to the surface, but these localized areas had been repaired.

This inspection was performed 12 to 40 years after the construction of these tanks. For this analysis it is assumed that the concrete remains in good condition. If desired, a second inspection prior to tank closure may be performed to confirm this assumption.

Figure 2-8. Concrete Vault for Type III Waste Tanks [2]

3.0 Corrosion Degradation Mechanisms for Steel Liner

3.1 Corrosion in Anoxic Environments

Steel is thermodynamically unstable when it is exposed to oxygen and water. Corrosion, an electrochemical process, occurs and layers of iron oxide or iron hydroxide form at the interface of the steel and the concrete. However, cementitious materials have two beneficial characteristics that mitigate corrosion when in intimate contact with steel. The concrete/grout is a porous material that limits the access of water and oxygen. The reduction in the access for oxygen creates an anoxic environment. The second beneficial aspect is that the cement paste is very alkaline (pH 11.5-13.5) and thus the corrosion products that do form are very insoluble. They produce a very thin protective coating, typically magnetite (Fe_3O_4), that reduces the corrosion rate to 0.1 to 1 μm/yr (0.04 mils/yr). The metal surface is typically referred to as passive.

An example of the magnetite film is shown in Figure 3-1. A leak detection box (LDB) in H-area had failed due to corrosion. The LDB was removed from service and brought to SRNL for a failure analysis [38]. The LDB has dip tube pipes that begin above grade and then penetrate through concrete and then soil to the box. The figure shows the above grade pipes and the pipes embedded in the concrete. The above grade pipes showed evidence of surface corrosion, while the embedded pipes had a thin black layer of magnetite (see section marked A). The area marked "A" had negligible corrosion after approximately 20 years of exposure.

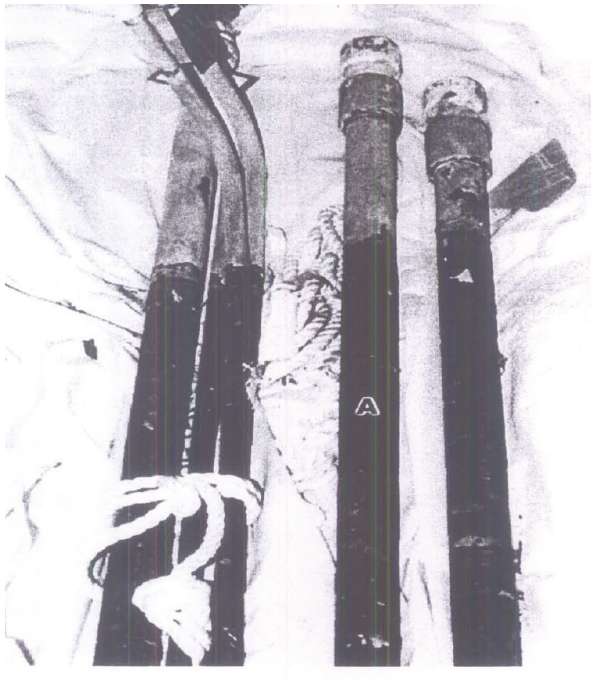

Figure 3-1. Leak detection box dip tubes; Section marked 'A' was submerged in concrete.

Theoretical models of the quantity of corrosion needed to cause cracking of the concrete assume that the corrosion products are voluminous, insoluble iron oxides (e.g., lepidocrocite, γ-FeO(OH)) and that they are always at the interface between the steel and the concrete. These assumed oxides are approximately six times as voluminous as the steel and promote cracking of the concrete. Observations of the corrosion products that form on embedded steel in the anoxic, passive condition indicate that they are a mixture of magnetite and other iron oxides that have a specific volume between 2.2 to 3.3 times the specific volume of the steel. The corrosion products also tend to precipitate in the concrete pores rather than always remaining at the interface between the concrete and the steel. Therefore, concrete degradation due to anoxic, or passive, corrosion is less than that compared with other mechanisms (e.g., chloride induced corrosion).

Corrosion of steel exposed to concrete/grout occurs by a complex mechanism through metal dissolution at the concrete/metal interface. This interfacial chemistry is controlled by the initial

construction characteristics and the grout formulations. In general, high quality concrete prevents corrosion of the steel by: (1) forming a passive oxide on the steel surface, (2) maintaining a high pH environment, and (3) providing a matrix resistant to diffusion of aggressive species. The passivity of the steel at the interface can be controlled by the dynamic characteristics of the "pore water" (interstitial solution) within the concrete [39]. The passivity is maintained at the high pH environments in the region of water stability. However, as pore water characteristics change with the introduction of chlorides or carbon dioxide, the passive film on the steel may break down. The two major causes of corrosion of steel exposed to concrete are carbonation and chloride induced breakdown of the passive film. The passivity of the steel is lost when the pH is lowered below 9 (by carbonation) or a critical chloride concentration is reached at the concrete metal interface [40]. These mechanisms will be discussed in more detail in subsequent sections of this report.

The passive film does not form immediately but rather initiates as soon as the pH of the mixing water rises in the concrete when the cement begins to hydrate and then cures during the first week [41]. Thus, for this case, it may be assumed that a passive layer forms on the steel surface spontaneously when in contact with the alkaline cement. The corrosion rate in this passive state is estimated to be 0.04 mils/year (1 μm/year). [42] This corrosion rate corresponds to a passive current density (I_{corr}) of 0.09 μA/cm^2, which is just below the typical threshold used for the passive state (i.e. I_{corr} < 0.1 μA/cm^2) [43]. Recent tests in anoxic, concrete pore water conditions indicated that the passive corrosion rates were on the order of 0.1 μm/year to 0.5 μm/year, which is consistent with these values [44]. Thus, the 1 μm/year value remains conservative.

3.2 Contamination zone

Corrosion of the steel exposed to the contamination zone, which is principally the area covered by the remaining heel of waste that was not removed from the tank bottom during waste retrieval, is a function of the chemistry of the undissolved solids in the residual on the tank bottom. Corrosion of the steel exposed to the contamination zone is most susceptible to nitrate induced corrosion. During corrosion in nitrate solutions, carbon steel reacts anodically by:

$$3Fe + 8OH^- = Fe_3O_4 + 4H_2O + 8e^- \qquad \text{Equation 3}$$

The cathodic reaction may be either oxygen or nitrate reduction depending on the availability of oxygen.

$$O_2 + 2H_2O + 4e^- = 4OH^- \qquad \text{Equation 4}$$

$$NO_3^- + H_2O + 2e^- = NO_2^- + 2OH^- \qquad \text{Equation 5}$$

However, because the tank is below grade and interstitial liquid is concentrated with sodium salts, thus limiting the dissolved oxygen concentration, oxygen availability to the contamination

zone is limited and therefore the environment is anoxic. In this situation, nitrate reduction is the more likely cathodic reaction. This reaction is slowed in the presence of a significant concentration of nitrite and hydroxide. For many years, the SRS tank farm facility utilized nitrite and hydroxide as corrosion inhibitors [33].

The free hydroxide concentration and the pitting factor, and a ratio of the inhibitor species (hydroxide and nitrite) to the aggressive species (nitrate, chloride, and fluoride), were used to assess the potential corrosivity of the contamination zone [45]. The free hydroxide concentration allows for an assessment of passivity of the carbon steel surface, while the pitting factor allows for an assessment of whether carbon steel is susceptible to localized corrosion due to aggressive species. If the free hydroxide concentration is greater than or equal to 0.01 M the surface remains passive and the corrosion rate is very low. In combination, with the magnetite on the surface (see anodic reaction) the general corrosion rate would be 0.04 mils/year (1 μm/year). If the pitting factor is less than 1, the passive film may break down and localized corrosion ensue. A higher rate of corrosion, 0.4 mpy, would be assumed in this case.

The expected residual material inventory was used to calculate the free hydroxide concentration and the pitting factor for the chemistry in the contamination zone, under the conservative assumption that the dried solids were in solution [46], [47].

$$A_{chemical}(M) = \frac{M_{solute}(g)}{g\ sludge} x \frac{885\ g\ sludge}{gal\ sludge} x \frac{Volume(gal)}{3.785\ l\ sludge} x \frac{1}{MW\ solute} \qquad \text{Equation 6}$$

where:

Density of Residuals = 885 g sludge/gal sludge [46], [47]

MW = Molecular Weight of Solute Anion (NO_3^- = 62 g/mole, OH^- = 40 g/mole, Cl^- = 35.5 g/mole, F^- = 17 g/mole)

The free hydroxide and pitting factor for each tank in F-Area are shown in Table 3-1 through Table 3-4. The free hydroxide and pitting factor for each tank in H-Area are shown in Table 3-5 through Table 3-9. Only two of the Type IV tanks, Tank 19 in F-Area and Tank 23 in H-Area, do not meet the criteria for the low passive corrosion rate. However, since both tanks were caustic during service and met the criteria for the corrosion control program during their service life, the presence of a protective magnetite film is likely. Thus, the low general corrosion rate of 1 μm/yr (0.04 mpy) will be assumed.

Table 3-1. Pitting Factor and Free Hydroxide Values for F-Area Type I Tanks

Tank #	1	2	3	4	5	6	7	8	Average
Pitting Factor	3.08	2.27	2.29	7.75	2.96	13.70	1.69	1.96	4.46
Free Hydroxide (M)	0.20	0.22	0.20	0.20	0.25	0.16	0.26	0.23	0.21

Table 3-2. Pitting Factor and Free Hydroxide Values for F-Area Type III Tanks

Tank #	33	34	Average
Pitting Factor	2.39	13.72	8.06
Free Hydroxide (M)	0.19	0.18	0.18

Table 3-3. Pitting Factor and Free Hydroxide Values for F-Area Type IIIA Tanks

Tank #	25	26	27	28	44	45	46	47	Average
Pitting Factor	1.55	1.55	1.55	1.55	1.55	1.55	1.55	1.55	1.55
Free Hydroxide (M)	0.24	0.24	0.24	0.24	0.24	0.24	0.24	0.24	0.24

Table 3-4. Pitting Factor and Free Hydroxide Values for F-Area Type IV Tanks

Tank #	17	18	19	20	Average
Pitting Factor	2.21	2.22	0.61	2.21	1.81
Free Hydroxide (M)	0.71	0.27	0.01	0.72	0.43

Table 3-5. Pitting Factor and Free Hydroxide Values for H-Area Type I Tanks

Tank #	9	10	11	12	Average
Pitting Factor	1.53	1.53	1.64	2.04	1.68
Free Hydroxide (M)	0.24	0.20	0.17	0.13	0.19

Table 3-6. Pitting Factor and Free Hydroxide Values for H-Area Type II Tanks

Tank #	13	14	15	16	Average
Pitting Factor	1.22	3.55	1.79	1.79	2.09
Free Hydroxide (M)	0.25	0.19	0.12	0.12	0.17

Table 3-7. Pitting Factor and Free Hydroxide Values for H-Area Type III Tanks

Tank #	29	30	31	32	Average
Pitting Factor	1.22	1.22	1.22	2.19	1.46
Free Hydroxide (M)	0.25	0.25	0.25	0.20	0.24

Table 3-8. Pitting Factor and Free Hydroxide Values for H-Area Type IIIA Tanks

Tank #	35	36	37	38	39	40	41	42	43
Pitting Factor	2.36	1.22	1.22	1.09	1.80	2.36	1.22	1.22	1.09
Free Hydroxide (M)	0.21	0.25	0.25	0.20	0.24	0.21	0.25	0.25	0.20
Tank #	48	49	50	51	Average				
Pitting Factor	1.22	1.22	1.22	2.36	1.51				
Free Hydroxide (M)	0.25	0.25	0.25	0.21	0.23				

Table 3-9. Pitting Factor and Free Hydroxide Values for H-Area Type IV Tanks

Tank #	21	22	23	24	Average
Pitting Factor	1.08	1.08	0.00	1.09	0.82
Free Hydroxide (M)	0.33	0.26	0.00	0.20	0.20

The anoxic, passive corrosion rates will be utilized as inputs for the corrosion of the embedded rebar and the steel associated with the primary and secondary liners, the column plates, and the cooling coils that are in contact with either grout or concrete, or the contamination zone. The mechanism will be assumed to result in uniform general corrosion of the steel.

Release of contaminants to the environment is predicated on complete degradation of the concrete and steel. Complete penetration of the primary and secondary liners was utilized as the failure time for the steel. The failure time is calculated by assuming the nominal thickness of a plate and dividing it by the anoxic corrosion rate.

$$\text{Failure Time} = \text{Nominal Thickness}/\text{Annual Corrosion Rate} \qquad \text{Equation 7}$$

It should be noted that this failure time may be accelerated by other corrosion mechanisms. For example, the interior of the secondary liner may be corroding due to anoxic corrosion, while the

exterior may be corroding by carbonation. Section 7.0 describing the approach to the progression model will illustrate how these mechanisms are coupled.

The embedded steel rebar will also corrode by anoxic, passive corrosion and this mechanism will contribute to the degradation of the concrete vault. The ACI 318 code was consulted to determine the minimum areal fraction of rebar that must be present for a given cross section of concrete [48]. For this analysis, if the fraction is less than 0.0018, the concrete structure will be considered to have failed. The calculations below take into account two rows of rebar, one on the exterior of the concrete vault and the second on the interior of the vault.

The following steps were performed to determine the time to failure for the concrete vault due to anoxic corrosion of the rebar.

1. Review drawings for each type of tank to determine the following:
   - The highest stress region for the roof, sidewall, and floor.
   - The diameter of the rebar utilized in this region (D, in).
   - The spacing between the rebar in this region (s, in.).
   - The wall thickness of the roof, sidewall, and floor (B, in.).
2. Determine the minimum area of rebar required (A, in^2).

$$A = \frac{B\ x\ s * 0.0018}{2} \qquad \text{Equation 8}$$

3. Calculate the minimum allowable rebar diameter (d, in).

$$d = \sqrt{\frac{4\ x\ A}{\pi}} \qquad \text{Equation 9}$$

4. Calculate the time, t in years, for the vault to fail due overload.

$$t = \frac{(D-d)}{4x\ 10^{-5}} \qquad \text{Equation 10}$$

The rebar sizes and spacing for each tank type and location were summarized in Section 2.0. Table 3-10 shows the anticipated time for failure due to rebar corrosion for each tank type and location. This time will be compared to the failure time for the concrete due to other mechanisms (e.g., carbonation). If this time is the minimum value, this will be utilized as the cut-off value for concrete degradation. This approach and how it is coupled to the overall time to failure of the concrete vault and the tank steel will be further amplified in Section 7.0 as the approach to the calculations is described.

3.3 Carbonation

In moist environments, carbon dioxide present in the air forms an acid aqueous solution that can react with hydrated cement paste in the concrete. This process, known as carbonation, tends to neutralize the alkalinity of concrete [49]. The alkaline constituents of concrete are present in the pore water (mainly as sodium and potassium hydroxides), but also in the solid hydration products (e. g. $Ca(OH)_2$ or C–S–H). Calcium hydroxide is the hydrate in the cement paste that reacts most readily with CO_2. The reaction, which takes place in aqueous solution, may be written:

$$Ca(OH)_2 + H_2O + CO_2 \leftrightarrow CaCO_3 + 2H_2O \qquad \text{Equation 11}$$

Carbonation does not cause any damage to the concrete itself, although it may cause the concrete to shrink. However, carbonation has important effects on corrosion of any embedded steel, notably rebar. The primary consequence is that the pH of the pore solution drops from its normal values of pH 13 to 14, to values less than 9 to 10 [50]. If chlorides are not present in concrete initially, the pore solution following carbonation is composed of almost pure water. This means that the steel in humid carbonated concrete corrodes as if it was in contact with water [49].

Table 3-10. Concrete Vault Failure Time Due to Anoxic, Passive Corrosion of Rebar for Each Tank Type and Location.

Type	Location	time (years)
I	Roof	11002
	Sidewall	10809
	Floor	9178
II	Roof	21341
	Sidewall	16373
	Floor	22983
III/IIIA	Roof	20884
	Sidewall	20393
	Floor	17228
IV	Roof	4742
	Sidewall	8021
	Floor	5418

The carbonation reaction starts at the external surface and penetrates the concrete producing a low pH front. The rate of carbonation decreases in time, as CO_2 has time to diffuse through the pores of the already carbonated outer layer. The penetration in time of carbonation can be described by:

$$d = A\sqrt{t} \qquad \text{Equation 12}$$

where d is the depth of carbonation (mils) and t is time (yrs), A is a carbonation constant to be determined. The rate of carbonation is influenced by environmental conditions such as humidity, temperature, and carbon dioxide concentration. Concrete composition (e.g., water/cement ratio) also plays a significant role in the rate of carbonation. The carbonation coefficient A (in/yr$^{1/2}$) can then be assumed as a measure of the rate of penetration of carbonation for given concrete and environmental conditions. A carbonation profile transient for each type of tank and location was determined by Flach [10]. The time to reach various steel plates (e.g., exterior of the secondary liner) was calculated. These times were utilized to determine the time to initiate carbonation. At that time, the passive layer on the steel breaks down and corrosion ensues.

The corrosion is general, like anoxic, and relatively homogeneous. The corrosion products, iron carbonates, are also more soluble in the neutral carbonated zone and diffuse to the surface of the concrete. Thus, the concrete does not tend to crack in this mechanism. The corrosion rate in carbonated concrete is greater than that for anoxic corrosion. For foundations and below grade concrete that are exposed to wet conditions, the corrosion rates range from 0.1 μA/cm^2 to 0.5 μA/cm^2 [51]. The higher corrosion rate will be utilized for this analysis, which is approximately 0.23 mpy.

The mechanism will be assumed to result in uniform general corrosion of the steel. Release of contaminants to the environment is predicated on complete degradation of the concrete and steel. Complete penetration of the primary and secondary liners was utilized as the failure time for the steel. The failure time is calculated by assuming the nominal thickness of a plate and dividing it by the anoxic corrosion rate.

$$\text{Failure Time} = \text{Nominal Thickness}/\text{Annual Corrosion Rate} \qquad \text{Equation 13}$$

It should be noted that this failure time may be accelerated by other corrosion mechanisms. For example, the interior of the secondary liner may be corroding due to anoxic corrosion, while the exterior may be corroding by carbonation. The section describing the approach to the progression model will illustrate how these mechanisms are coupled.

3.4 Chloride/O2

Chloride contamination of concrete is a frequent cause of corrosion of reinforcing steel [52]. There are two primary sources of chloride. The first is the fresh concrete itself. In the past chlorides were unknowingly or deliberately added to the concrete in the form of contaminated

water, aggregates or accelerating admixtures. A review of the concrete that was utilized for the SRS waste tanks indicated that the chloride levels in the concrete are expected to be low [12]. In a related study, a chip of concrete from a Type III Tank roof exterior surface was analyzed for chloride. The total chloride concentration was determined to be 5 ppm [53]. Thus, the concrete mix is not anticipated to be a significant source of chloride.

The other main source of chloride in concrete is penetration from the environment, in this case primarily from the surrounding soil or the atmosphere above the roof. This occurs, for instance, in marine environments or in road structures in regions where chloride-bearing de-icing salts are used in wintertime.

Chlorides lead to a local breakdown of the protective oxide film on the reinforcement in alkaline concrete, so that a subsequent localized corrosion attack takes place. Areas no longer protected by the passive film act as anodes (active zones) with respect to the surrounding still passive areas where the cathodic reaction of oxygen reduction takes place. The morphology of the attack is that typical of *pitting*. Once corrosion has initiated, a very aggressive environment will be produced inside pits. Due to the presence of oxygen, voluminous iron oxides (~ 6 times the specific volume of the steel) precipitate and form at the steel concrete interface, which results in cracking of the concrete.

The time to initiation depends on the rate at which the chloride ions penetrate the surface. Time-dependent diffusion equations may be solved analytically to illustrate the diffusion of chloride ions through a concrete structure [10]. The differential equations used to model chloride diffusion through the concrete slabs are:

$$\frac{\partial c_{Cl}}{\partial t} = D_{Cl}\frac{\partial^2 c_{Cl}}{\partial x} \qquad \text{Equation 14}$$

where: c_{Cl} = Chloride concentration in concrete (ppm),

D_{Cl} = Chloride ion diffusion coefficient (cm^2/s),

t = Time (s), and

x = Distance into slab from outside (cm).

The solution to this equation is:

$$c_{Cl} = c_{0,Cl}\left[1 - erf\left(\frac{x}{2\sqrt{D_{Cl}t}}\right)\right] \qquad \text{Equation 15}$$

where: $c_{0,Cl}$ = Chloride concentration in concrete/soil interface (ppm).

Corrosion of reinforcement in non-carbonated concrete can only take place once the chloride content in the concrete in contact with the steel surface has reached a threshold value [54]. This threshold chloride concentration depends on several parameters such as concentration of hydroxide ions in the pore water, binder type, surface condition of the steel, chloride source, oxygen availability at the steel surface. There are two principal expressions of the threshold chloride: the [Cl-]/[OH-] ratio and the total chloride relative to the weight of the cement. The former ratio was recommended by Hausmann [55] in the late 1960's and was determined by tests in pore water solution to be approximately 0.6. The second ratio is more common since measurement of the total chloride is relatively simple and well accepted by standards [54]. A typical value accepted by the American Concrete Institute (ACI) is 0.4 wt.%.

However, a recent review of the critical chloride content demonstrated that there is no general agreement on the critical chloride threshold (i.e., there is wide range of values presented in the literature) [54]. The disagreement is primarily due to inconsistencies in the laboratory testing, non-representative experiments, and the statistical nature of pitting. In addition, structures that are submerged and have a moisture content of the concrete that is near saturation will have a limited amount of oxygen transported through the concrete to the steel [10]. Thus, the threshold chloride concentration may increase by as much as an order of magnitude as compared with an above-ground structure [52]. That said, the Hausmann ratio for pore water and the ACI ratio for total chloride appear to be appropriate lower bounds to evaluate the likelihood of the initiation of pitting.

The corrosion rate can be calculated by relating oxygen diffusion through the concrete to the corrosion reaction. As a conservative assumption, the rebar will be considered to corrode uniformly. The overall corrosion reaction is:

$$Fe + \frac{3}{2}H_2O + \frac{3}{4}O_2 \leftrightarrow Fe(OH)_3 \qquad \text{Equation 16.}$$

The oxygen diffusion through the concrete is represented by:

$$N_{O_2} = D_{O_2}\frac{C_{gw}}{\Delta X} \qquad \text{Equation 17}$$

where: N_{O_2} = Flux of O_2 through the Concrete (mol/s/cm^2),

D_{O_2} = Diffusion Coefficient for O_2 in Concrete (cm^2/s),

C_{O_2} = Dissolved Oxygen in Groundwater (mol/cm^3), and

ΔX = Concrete Thickness (cm).

The corrosion rate can then be calculated by:

$$R_{corrosion} = \frac{4}{3} N_{O_2} \frac{M_{Fe}}{\rho_{Fe}} \qquad \text{Equation 18}$$

where: $R_{corrosion}$ = Corrosion Rate (cm/s)

M_{Fe} = Molecular Weight of Iron (56 g/mol), and

ρ_{Fe} = Density of Iron (7.86 g/cm^3).

Flach calculated oxygen profile transients [10] to assess the corrosion rate of the steel due to this mechanism.

The chloride concentration present in SRS soil is on the order of 2 ppm. Flach calculated the maximum chloride concentration in the concrete vault wall is 5.64 x 10^{-5} M [10]. The weight of the cement in the concrete that was used for the concrete vault was nominally 520 lb/yard^3. If the total chloride is at the threshold of 0.4% of the cement by weight, this is equivalent to 3.5 x 10^{-2} M. Thus, by this criterion, and considering that this is a below grade structure, it is very unlikely that chloride will depassivate the steel surface and initiate corrosion. Likewise, the hydroxide concentration in the pore water would need to decrease to 9.4 x 10^{-5} M, or a pH slightly below 10, for the threshold ratio of 0.6 to be exceeded. This is approximately the same pH that would initiate corrosion by carbonation. However, given the anticipated low oxygen concentration in the concrete vault the corrosion rate due to oxygen, as calculated by Equation 18, the corrosion rate is several orders of magnitude less than that observed for carbonation. Thus, this mechanism of failure seems unlikely.

This conclusion differs from previous steel liner evaluations [6] [7]. However, those previous evaluations utilized a higher initial chloride concentration (10 ppm) and assumed an empirical relationship, typically applied to bridge decks where sufficient oxygen is present, to calculate the initiation time. The result was a shorter initiation time for chloride induced corrosion. The calculations also assumed an upper bound diffusion rate coefficient for oxygen. Even with this assumption, the corrosion rate barely exceeded the anoxic, passive corrosion rate for steel. Recent calculations by Flach confirmed this result [10]. Therefore, this mechanism was not considered in this report.

3.5 Indoor Air

For the Compliance and Pessimistic Cases, gaps between the grout and the roof (Pessimistic Case only) or the sidewalls of the tanks are postulated to exist. In the early stages, before the concrete degrades completely, the steel remains relatively protected from the soil environment.

The air in these gaps likely has a low level of contaminants (e.g., chlorides and sulfates) and low levels of radiation dose, and ambient temperatures (e.g., 15-20 ºC) and relative humidity levels on the order of 70-100%. This environment is similar to the corrosion conditions considered for carbon steel packages stored under indoor conditions [56] [57]. The average corrosion rate for carbon steel at indoor conditions was approximately 0.4 mpy over a 3-year period [57] (see Figure 3-2). This rate will be extrapolated to longer time periods and is considered bounding. The corrosion occurs uniformly over the surface of the steel.

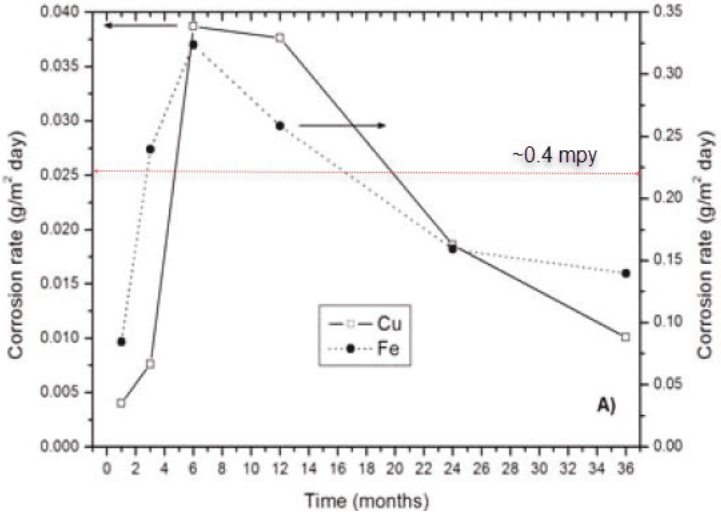

Figure 3-2. Indoor air corrosion rate for carbon steel. The red line shows an average corrosion rate that has been converted from g/m^2/day to mils/yr [57].

The indoor air corrosion rate will be utilized to assess the situation when a gap exists between the poured grout and prior to the concrete degrading completely. Failure of the steel occurred when corrosion penetrates the thickness of the steel.

3.6 Humid Air

The life of the tank steel was also estimated for a condition in which a gap of humid air may form between the grout/vault and the tank steel. This situation differs from the indoor air condition in that the concrete has completely degraded and the vault is no longer protecting the steel from the exterior conditions. This configuration could form due to shrinkage of the grout or corrosion of the transfer line that penetrates through the sidewall of the tanks. Humid air corrosion in the tanks can be modeled as analogous to damp atmospheric corrosion that occurs due to the formation of thin electrolyte layers on a metal surface leading to corrosion with any contaminants (e.g. NaCl, Na_2SO_4), leading to increased corrosion rates. Although this critical humidity level may vary depending upon the temperature, environmental pollutants, and the metal exposed, it is assumed that the critical humidity is always maintained for these calculations. In addition, it is assumed that there are no contaminants of consequence in any

humid air exposed to the tank surface. The corrosion of the tank steel under thin films proceeds with the anodic reaction being the dissolution of the metal and the cathodic reaction being the oxygen reduction reaction. It is important to recognize that oxygen is always available for thin films and diffusion through the thin films is relatively fast.

Data obtained for the Yucca Mountain Project (YMP) is appropriate for this analysis. The corrosion testing in support of the YMP project included exposing A516 Gr. 55 coupons to the vapor space above simulated dilute water (SDW) for a year of exposure at 60 and 90°C [58]. The data for the vapor space corrosion of the coupons indicated a higher corrosion rate than that of the aqueous exposure potentially due to the carbon dioxide evolution from the carbonate in the solution. The data is shown in Table 3-11.

Table 3-11. Corrosion rates of vapor space coupons in Yucca Mountain study.

Solution	Temperature	Corrosion Rate			
		6-month test		12-month test	
		(μm/yr)	(mpy)	(μm/yr)	(mpy)
SDW	60°C	46	1.8	27	1.06
SDW	90°C	77	3.03	56	2.2

For this analysis, the average corrosion rate of 51.5 μm/yr (or 2.03 mpy) was assumed. This corrosion rate is likely bounding as the temperatures will likely be lower in the tank vault. Uniform corrosion of the steel was also assumed.

The humid air corrosion rate will be utilized to assess the situation when the concrete vault has failed, and a fast flow path exists for the exterior air to reach the steel surface. Failure of the steel occurred when corrosion penetrates the thickness of the steel.

3.7 Groundwater

Exposure of sections of steels to groundwater can increase corrosion susceptibility and variation of groundwater exposure levels can further increase corrosion due to the variation in aeration. Two conditions would need to occur for this scenario. First, the concrete would need to completely degrade, which would allow groundwater to flow freely to the steel. Secondly, a tank component would need to be located at or below the water table. To quantify corrosion rates of steels in groundwater, National Bureau of Standards data was used [59]. The NBS soil type with the highest moisture content and having a pH similar to SRS soil was muck from New Orleans, LA. The characteristics of this soil are shown in Table 3-12:

Table 3-12. Muck soil conditions used for groundwater corrosion modeling.

Soil Property	Value
Location	New Orleans, LA
Type of Soil	Muck
Annual Precipitation	57.4 in.
Resistivity	712Ω-cm
pH	4.8
Temperature	69.3 °F
Moisture Equivalent	57.8 %

The weight-loss and maximum penetration data presented for open-hearth steel plate [59] was used to calculate the corrosion rate and maximum penetration rate (i.e. localized corrosion rate). The results are shown in Table 3-13 and corrosion data are graphed in Figure 3-3. The initial general corrosion rate is 4 mpy, which decays with time due to the build-up of oxides.

Table 3-13. Weight loss of steel in groundwater.

Year	Weight Loss		Corrosion Rate		Maximum Penetration	
	(oz/ft^2)	(kg/m^2)	(mils/yr)	(mm/yr)	(mils/yr)	(mm/yr)
2.1	5.7	1.74	4.15	105.51	14.76	374.95
4	9.9	3.02	3.79	96.21	15.25	387.35
8.9	16.9	5.16	2.91	73.82	10.00	254.00
11.2	17.2	5.25	2.35	59.70	14.38	365.13
12.7	18.1	5.52	2.18	55.40	14.80	376.00

A corrosion rate of 2.0 mils/year may be assumed as an estimate of the long-term general corrosion rate for tank steel exposed to ground water. The corrosion rate appears to asymptotically approach this value after 12 years of exposure. The value is non-conservative with respect to the amount of steel wall loss initially, however, with time it may become more conservative if the corrosion rate continues to decay.

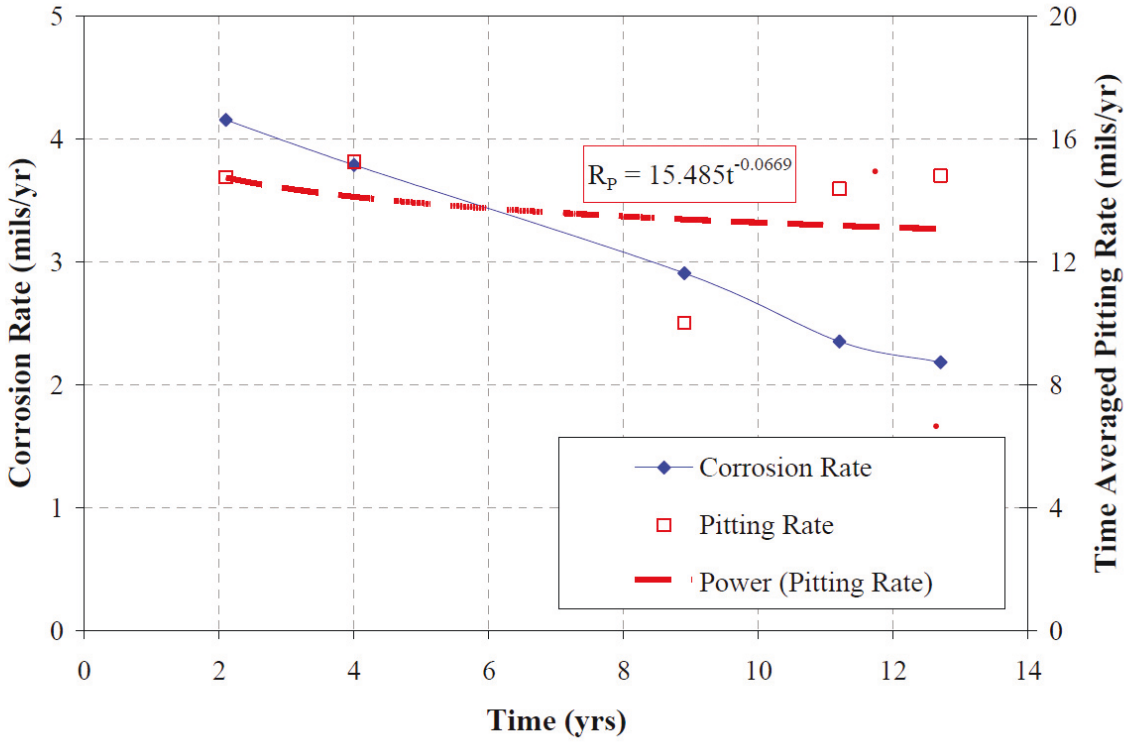

Figure 3-3. Corrosion rate and penetration rate for carbon steel in groundwater.

Pitting occurs in broad, shallow patches on the surface that eventually coalesce and penetrate through wall. The rate at which this occurs is typically faster than general corrosion. A pitting model developed by Sullivan was utilized to estimate the time for pitting to breach the tank wall [60]. The pitting model assumes formation of a hemispherical pit and estimates the fraction of tank area breached based upon the maximum pit depth, the corrosion allowance, and the number of penetrating pits per container:

$$A_b = N_p \pi \left(h^2 - d^2 \right) \qquad \text{Equation 19}$$

where: A_b = Fraction of Area Pitted,

N_p = Penetrating Pits per Container (pits/m^2) – assumed to be 5000,

h = Maximum Pit Depth (m), and

d = Corrosion Allowance or wall thickness (m).

The maximum pit depth can be estimated by:

$$h = kt^n \left(\frac{A}{372} \right)^a \qquad \text{Equation 20}$$

where: k = Empirical Pitting Parameter (m/yr^n),

t = Corrosion Time (yr),

n = Empirical Pitting Exponent,

A = Representative Surface Area (cm^2); assumed to be 10,000, and

a = Experimentally Derived Experimental Coefficient.

Regression analysis of penetration rate data in Figure 3-3 [59] was used to determine the penetration rate as a function of time. The time averaged pitting rate was determined by integrating this function. This yielded values of 9.46 m/yr^n and 0.993 respectively for 'k' and 'n' shown in Equation 20 [61]. An average value of 0.15, as determined from the literature was utilized for exponent 'a' [62]. Using these values, the final form of the equation is:

$$h = 25.4t^{0.993} \qquad \text{Equation 21.}$$

where h is the maximum pit depth in mils. It was demonstrated previously that pitting corrosion for the groundwater case will proceed at much higher rate than general corrosion [7]. The pit depth regression fit shown in Equation 21 and the breach model equation shown in Equation 19, were utilized to predict the time to first pit penetration and the time to 25% breach of a given location (e.g., roof). The 25% criterion was used in the previous analysis to indicate that the steel had been severely compromised [6], [7].

4.0 Degradation Mechanisms for Concrete

4.1 Chemical and Physical Effects

Modeling of the chemical and physical degradation of the concrete materials of the tank vault was performed by SRR [10]. Data from these models was coupled to the progressive degradation models for the tank steel and rebar in this investigation. Much of the chemical evolution analysis was performed with equilibrium chemistry simulation software, namely The Geochemist's Workbench® (GWB) and PHREEQC®. Custom thermodynamic databases formatted for these codes were developed from Denham [3], CEMDATA18.1 [63], and ThermoChimie [64]. Initial simulations defined the equilibrium chemical state of SRS rainwater, soil moisture, groundwater, and hydrated grouts and concrete. Subsequent simulations predict the chemical evolution of the initially cured cementitious materials when subjected to long-term 1) successive pore volume flushes (advective transport) and 2) leaching to adjoining soil/sediment (diffusive transport). The principal results are pH and Eh variations in cement pore solutions as a function of pore volumes (advection) or time (diffusion).

The physical evolution analysis is based on simplified conceptual models (abstractions) that facilitate analytic mathematical solutions. A feedback mechanism is provided whereby physical damage to concrete predicted by reactive transport in turn affects species transport rates. Results for penetration depth in concrete as a function of time are generated for 1) carbonation and physical damage fronts, 2) decalcification and damage fronts, and 3) combined carbonation + decalcification and damage fronts. Methods for estimating 1) oxygen flux and cumulative mass transported and 2) chloride concentration were also developed. The results from the physical evolution analyses were used for the steel degradation analysis.

Methods, input values, and assumptions in the study generally represent a varying blend of best-estimate and pessimistic settings. Sensitivity case studies were performed in the chemical evolution analysis to provide a sense of model biases and uncertainties. For physical evolution, three cases representing varying conservatism are considered: Realistic Case, Compliance Case, and Pessimistic Case. The key parameters that were varied for the physical evolution calculations were: liquid saturation, gas-phase intrinsic diffusion coefficient, liquid-phase effective diffusion coefficient, apparent diffusion coefficient in the liquid, carbonation + dissolution rate constant, and damage front lag. Results from these calculations are shown in Section 6.0.

4.2 Structural Cracks

The physical evolution model generally did not assume the presence of initial structural cracks in the concrete vault, the exception being the concrete floor for the Pessimistic Case. Concrete exhibits excellent strength properties in compression, but cracks form when the monolith is in tension, flexure, or shear. To ensure that large beams can sustain these stresses rebar is added to the concrete monolith [65]. The presence of cracks shortens the corrosion initiation time for the steel and accelerates the corrosion rate during service life. The degree to which cracks influence corrosion is dependent upon the orientation of the crack, the crack width, crack frequency or spacing, crack depth, and concrete composition characteristics (e.g., admixtures such as fly ash). The most common cracks due to structural loads are referred to as transverse cracks as they run perpendicular to the rebar. Longitudinal cracks, which run parallel to the rebar, form after the corrosion of the rebar. These cracks are considered more dangerous than transverse crack because more of the steel area is exposed to the aggressive environment. However, for the initiation of corrosion, the transverse cracks are likely to play a larger role for the concrete vaults.

There have been many studies on the influence of crack geometry and spacing on corrosion of rebar [65], [66], [50], [67]. Although general principles regarding the effects are understood (e.g., corrosion increases with crack width and frequency), results from experiments show inconsistencies in the relationship between the propagation of the carbonation front in a cracked versus an uncracked concrete due to the variation in the experimental approaches. The ratio of the rate of penetration of the carbonation front for cracked versus uncracked concrete ranged

between 2 to 10. Given that carbonation is one of the mechanisms of concern, data from a source relative to that mechanism was considered [50]. The experimental data was input into a service life model developed by the authors. The model predicted that the carbonation depth for the cracked concrete would be three times greater than that for an uncracked sample. This value, although it is perhaps on the low end, is within the range observed by other authors and was performed for the carbonation mechanism. Thus, for this assessment, structural cracks will be assumed to increase the diffusion rate of the aggressive species by a factor of three.

The other aspect to consider in this evaluation is the location of the highest tensile, flexure or shear stress. Typically for the concrete tank vaults the highest stress occur in one of two places: 1) near the corner of where the floor and the sidewall intersect, and 2) on the floor beneath column supports. An increase in the density of rebar (i.e., smaller spacing and thicker diameter bars) is typically seen in these areas. For this investigation to demonstrate the effect of structural cracks on the projected service life, it was assumed that the greatest crack density was on the floor or the foundation. Thus, for the Pessimistic Case the gas diffusion coefficients for the floor were increased by a factor of three compared to the sidewall to account for postulated cracks, although none have been observed.

5.0 Model Cases for Long-Term Environment

The Performance Assessment considers many cases to investigate predicted and postulated scenarios. For tank vault degradation four cases were investigated: Central Scenario Realistic Case, Central Scenario Compliance Case, Central Scenario Pessimistic Case, and Fast Flow Path Case [10]. The Realistic Case utilizes best estimate or mean value data; the Pessimistic Case typically assumes worst-case bounding estimates on the data; and the Compliance Case typically is an average of the Realistic and Pessimistic Cases. The result is that the release times are spread out over time.

Within each case both saturated and vadose zone conditions were considered. For the saturated zone, gases such as carbon dioxide and oxygen diffuse through the liquid phase only. For the vadose zone conditions, void spaces exist that allow the gases to diffuse at a more rapid rate. Thus, corrosion of the steel and degradation of the concrete proceed at a more rapid rate. Finally, once the concrete degrades completely, groundwater penetrates the tank vault under the saturated zone, while for the vadose zone humid air conditions exist.

The Fast Flow Path Case was performed to demonstrate how quickly the steel corrodes if the concrete and grout are degraded and provide no protection for the steel. This sensitivity case is not postulated for design or compliance purposes, but rather illustrates how the concrete vault protects the steel and enables long periods for a barrier for the contamination zone to exist.

Based on the scenario descriptions, the initial condition of the steel after grouting can be established. The table associated with each case describes where the plate is located and specifies the environment each side, interior or exterior, is exposed. The exterior side is always

the side closest to the tank vault. Furthermore, the initial corrosion mechanism for each case is defined.

5.1 Realistic Case

1. As-designed construction of tank and closure process.
    a. No voids/gaps/cold joints in tank, annulus, and cooling coil grouts
    b. No fast-flow paths through concrete at construction joints, risers, and transfer lines
    c. Waste tank internal support structures (columns) intact
    d. All internal failed vertical pump assemblies and annulus ductwork were grouted (all tanks)

2. Minimal concrete/grout degradation
    a. Concrete degrades due to failure of rebar that corrodes by anoxic corrosion
    b. Concrete degrades due to penetration of gases

Table 5-1 through Table 5-4 represent the steel plate initial condition in both the saturated and vadose zones for each tank type. There are three environments considered: concrete, grout, and contamination zone. The mechanism for the concrete and grout was assumed to be anoxic, passive corrosion, while the mechanism for the contamination zone was general corrosion and the rate would be low. The rates for each mechanism were discussed in Section 4.0.

5.2 Compliance Case

1. Adequate construction and closure
    a. No voids/gaps in tank and annulus grouts along floor and wall, but a gap exists between the roof liner and tank-fill grout
    b. Cold joints in tank and annulus grouts
    c. Cooling coils not totally grouted but no vertical connection; steel intact
    d. Localized primary liner holes where already observed and/or postulated (more holes)
    e. Localized secondary liner holes where already observed and/or postulated (more holes)
    f. No Fast-flow paths through concrete at construction joints, risers, and transfer lines
    g. Waste tank internal support structures (columns) intact
    h. Internal failed vertical pumps and annulus ductwork not totally grouted but no vertical connection (all tanks)
2. Expected concrete/grout degradation
    a. Concrete degrades due to failure of rebar that corrodes by anoxic corrosion
    b. Concrete degrades due to penetration of gases.

The steel plate initial conditions in saturated and vadose zones for the Compliance Case are the same as those for the Realistic Case. Thus, the tables shown in the previous section will be utilized as inputs. The evolution of concrete degradation is different for the Compliance Case as will be shown in Section 8.0.

Table 5-1. Initial Conditions for Realistic Case Type I Tanks

	Location	Interior/Exterior	Environment	Mechanism
Type I Tanks	Roof Primary	Interior	Grout	Anoxic
		Exterior	Concrete	Anoxic
	Sidewall Secondary	Interior	Grout	Anoxic
		Exterior	Concrete	Anoxic
	Sidewall Primary	Interior	Grout	Anoxic
		Exterior	Grout	Anoxic
	Floor Primary	Interior	Contamination Zone	Low, general
		Exterior	Grout	Anoxic
	Floor Secondary	Interior	Contamination Zone	Low, general
		Exterior	Concrete	Anoxic

Table 5-2. Initial Conditions for Realistic Case Type II Tanks

	Location	Interior/Exterior	Environment	Mechanism
Type II Tanks	Roof Primary	Interior	Grout	Anoxic
		Exterior	Concrete	Anoxic
	Sidewall Secondary	Interior	Grout	Anoxic
		Exterior	Concrete	Anoxic
	Sidewall Primary (Top Knuckle/Top Plate)	Interior	Grout	Anoxic
		Exterior	Grout	Anoxic
	Sidewall Primary (Mid Plate)	Interior	Grout	Anoxic
		Exterior	Grout	Anoxic
	Sidewall Primary (Bottom Knuckle)	Interior	Contamination Zone	Low, general
		Exterior	Contamination Zone	Low, general
	Floor Primary	Interior	Contamination Zone	Low, general
		Exterior	Grout	Anoxic
	Floor Secondary	Interior	Contamination Zone	Low, general
		Exterior	Concrete	Anoxic

Table 5-3. Initial Conditions for Realistic Case Type III/IIIA Tanks

	Location	Interior/Exterior	Environment	Mechanism
Type III/IIIA Tanks	Roof Secondary	Interior	Grout	Anoxic
		Exterior	Concrete	Anoxic
	Roof Primary	Interior	Grout	Anoxic
		Exterior	Grout	Anoxic
	Sidewall Secondary	Interior	Grout	Anoxic
		Exterior	Concrete	Anoxic
	Sidewall Primary (Top Knuckle/Top Plate)	Interior	Grout	Anoxic
		Exterior	Grout	Anoxic
	Sidewall Primary (Mid Plate)	Interior	Grout	Anoxic
		Exterior	Grout	Anoxic
	Sidewall Primary (Bottom Knuckle Type IIIA)	Interior	Contamination Zone	Low, general
		Exterior	Grout	Anoxic
	Sidewall Primary (Bottom Knuckle Type III)	Interior	Contamination Zone	Low, general
		Exterior	Grout	Anoxic
	Floor Primary	Interior	Contamination Zone	Low, general
		Exterior	Grout	Anoxic
	Floor Secondary	Interior	Grout	Anoxic
		Exterior	Concrete Grout	Anoxic

Table 5-4. Initial Conditions for Realistic Case Type IV Tanks

	Location	Interior/Exterior	Environment	Mechanism
Type IV Tanks	Sidewall	Interior	Grout	Anoxic
		Exterior	Concrete	Anoxic
	Bottom Knuckle	Interior	Contamination Zone	Low, General
		Exterior	Concrete	Anoxic
	Floor	Interior	Contamination Zone	Low, General
		Exterior	Concrete	Anoxic

5.3 Pessimistic Case

1. Poor construction and closure
    a. No voids/gaps in tank and annulus grouts along floor
    b. Voids/gaps in tank and annulus grouts along roof and wall
    c. indoor air exists in gaps before complete degradation of tank vault
    d. Cold joints exist in tank and annulus grouts
    e. No grout within cooling coils; steel intact
    f. Localized primary liner holes where possible due to incomplete observation (many more holes)
    g. Localized secondary liner holes where possible due to incomplete observation (many more holes)
    h. Fast-flow paths through concrete at construction joints, risers, and transfer lines; groundwater or humid air flows through after concrete degrades
    i. Waste tank internal support structures (columns) initially degraded
    j. No grout within internal failed vertical pumps (all tanks)
2. Pessimistic Case concrete/grout degradation
    a. Concrete degrades due to failure of rebar that corrodes by anoxic corrosion
    b. Concrete degrades due to penetration of gases
    c. Concrete floor has structural cracks; Diffusion coefficient in the floor is 3 times greater than sidewall or roof

The initial conditions for the steel plates in the saturated and vadose zones for the Pessimistic Scenario, shown in Table 5-5 through Table 5-8, differ in one respect from the other two scenarios. In this case, it is postulated that shrinkage of the grout results in a "gap" of air existing between the grout and the sidewall and roof steel surfaces. The concrete is not degraded at this stage, so a corrosion rate represented of a sheltered, or protected atmospheric condition was assumed. This condition was referred to as indoor air and was described in greater detail in Section 4.0. This mechanism occurs uniformly over the steel at a rate that is accelerated compared to the concrete, grout, and contamination zone.

Table 5-5. Initial Conditions for Pessimistic Case Type I Tanks

	Location	Interior/Exterior	Environment	Mechanism
Type I Tanks	Roof Primary	Interior	Indoor Air	Accelerated, general
		Exterior	Concrete	Anoxic
	Sidewall Secondary	Interior	Indoor Air	Accelerated, general
		Exterior	Concrete	Anoxic
	Sidewall Primary	Interior	Indoor Air	Accelerated, general
		Exterior	Indoor Air	Accelerated, general
	Floor Primary	Interior	Contamination Zone	Low, general
		Exterior	Grout	Anoxic
	Floor Secondary	Interior	Contamination Zone	Low, general
		Exterior	Concrete	Anoxic

Table 5-6. Initial Conditions for Pessimistic Case Type II Tanks

	Location	Interior/Exterior	Environment	Mechanism
Type II Tanks	Roof Primary	Interior	Indoor Air	Accelerated, general
		Exterior	Concrete	Anoxic
	Sidewall Secondary	Interior	Indoor Air	Accelerated, general
		Exterior	Concrete	Anoxic
	Sidewall Primary (Top Knuckle/Top Plate)	Interior	Indoor Air	Accelerated, general
		Exterior	Indoor Air	Accelerated, general
	Sidewall Primary (Mid Plate)	Interior	Indoor Air	Accelerated, general
		Exterior	Grout	Anoxic
	Sidewall Primary (Bottom Knuckle)	Interior	Indoor Air	Low, general
		Exterior	Indoor Air	Low, general
	Floor Primary	Interior	Contamination Zone	Low, general
		Exterior	Grout	Anoxic
	Floor Secondary	Interior	Contamination Zone	Low, general
		Exterior	Concrete	Anoxic

Table 5-7. Initial Conditions for Pessimistic Case Type III/IIIA Tanks

	Location	Interior/Exterior	Environment	Mechanism
Type III/IIIA Tanks	Roof Secondary	Interior	Indoor Air	Accelerated, general
		Exterior	Concrete	Anoxic
	Roof Primary	Interior	Indoor Air	Accelerated, general
		Exterior	Indoor Air	Accelerated, general
	Sidewall Secondary	Interior	Indoor Air	Accelerated, general
		Exterior	Concrete	Anoxic
	Sidewall Primary (Top Knuckle/Top Plate)	Interior	Indoor Air	Accelerated, general
		Exterior	Indoor Air	Accelerated, general
	Sidewall Primary (Mid Plate)	Interior	Indoor Air	Accelerated, general
		Exterior	Indoor Air	Accelerated, general
	Sidewall Primary (Bottom Knuckle Type IIIA)	Interior	Indoor Air	Accelerated, general
		Exterior	Indoor Air	Accelerated, general
	Sidewall Primary (Bottom Knuckle Type III)	Interior	Indoor Air	Accelerated, general
		Exterior	Indoor Air	Accelerated, general
	Floor Primary	Interior	Contamination Zone	Low, general
		Exterior	Grout	Anoxic
	Floor Secondary	Interior	Grout	Anoxic
		Exterior	Concrete Grout	Anoxic

Table 5-8. Initial Conditions for Pessimistic Case Type IV Tanks

	Location	Interior/Exterior	Environment	Mechanism
Type IV Tanks	Sidewall	Interior	Indoor Air	Accelerated, general
		Exterior	Concrete	Anoxic
	Bottom Knuckle	Interior	Indoor Air	Accelerated, general
		Exterior	Concrete	Anoxic
	Floor	Interior	Contamination Zone	Low, General
		Exterior	Concrete	Anoxic

5.4 Fast Flow Path Case

1. Concrete and grout are completely degraded (or otherwise do not protect steel against environmental exposure and accelerated corrosion)
2. Voids and gaps exist at the roof, sidewall, and floor within the primary liner and annulus
3. Groundwater or humid air fills these gaps

The initial conditions for the steel plates in the saturated and vadose zones for the Fast Flow Path Case, shown in Table 5-9 through Table 5-12 for the saturated zone and Table 5-13 through Table 5-16 for the vadose zone, differ in one respect from the Pessimistic Case. Like the Pessimistic Case, it is postulated that shrinkage of the grout results in a "gap" of air existing between the grout and the sidewall and roof steel surfaces. However, in this Scenario the concrete has degraded completely, and the steel is exposed to either the soil groundwater (saturated zone) or humid air (vadose zone) immediately. Exposure to ground water will result in pitting corrosion, while the humid air is assumed to corrode generally at a very fast rate. These mechanisms were discussed in greater detail in Section 4.0.

Table 5-9. Initial Conditions for Fast Flow Case Type I Saturated Zone Tanks

	Location	Interior/Exterior	Environment	Mechanism
Type I Tanks	Roof Primary	Interior	Groundwater	Fast Flow, pitting
		Exterior	Groundwater	Fast Flow, pitting
	Sidewall Secondary	Interior	Groundwater	Fast Flow, pitting
		Exterior	Groundwater	Fast Flow, pitting
	Sidewall Primary	Interior	Groundwater	Fast Flow, pitting
		Exterior	Groundwater	Fast Flow, pitting
	Floor Primary	Interior	Contamination Zone	Low, general
		Exterior	Grout	Anoxic
	Floor Secondary	Interior	Contamination Zone	Low, general
		Exterior	Groundwater	Fast Flow, pitting

Table 5-10. Initial Conditions for Fast Flow Case Type II Saturated Zone Tanks

	Location	Interior/Exterior	Environment	Mechanism
Type II Tanks	Roof Primary	Interior	Groundwater	Fast Flow, pitting
		Exterior	Groundwater	Fast Flow, pitting
	Sidewall Secondary	Interior	Groundwater	Fast Flow, pitting
		Exterior	Groundwater	Fast Flow, pitting
	Sidewall Primary (Top Knuckle/Top Plate)	Interior	Groundwater	Fast Flow, pitting
		Exterior	Groundwater	Fast Flow, pitting
	Sidewall Primary (Mid Plate)	Interior	Groundwater	Fast Flow, pitting
		Exterior	Groundwater	Fast Flow, pitting
	Sidewall Primary (Bottom Knuckle)	Interior	Groundwater	Fast Flow, pitting
		Exterior	Groundwater	Fast Flow, pitting
	Floor Primary	Interior	Contamination Zone	Low, general
		Exterior	Grout	Anoxic
	Floor Secondary	Interior	Contamination Zone	Low, general
		Exterior	Groundwater	Fast Flow, pitting

Table 5-11. Initial Conditions for Fast Flow Case Type III/IIIA Saturated Zone Tanks

	Location	Interior/Exterior	Environment	Mechanism
Type III/IIIA Tanks	Roof Secondary	Interior	Groundwater	Fast Flow, pitting
		Exterior	Groundwater	Fast Flow, pitting
	Roof Primary	Interior	Groundwater	Fast Flow, pitting
		Exterior	Groundwater	Fast Flow, pitting
	Sidewall Secondary	Interior	Groundwater	Fast Flow, pitting
		Exterior	Groundwater	Fast Flow, pitting
	Sidewall Primary (Top Knuckle/Top Plate)	Interior	Groundwater	Fast Flow, pitting
		Exterior	Groundwater	Fast Flow, pitting
	Sidewall Primary (Mid Plate)	Interior	Groundwater	Fast Flow, pitting
		Exterior	Groundwater	Fast Flow, pitting
	Sidewall Primary (Bottom Knuckle Type IIIA)	Interior	Groundwater	Fast Flow, pitting
		Exterior	Groundwater	Fast Flow, pitting
	Sidewall Primary (Bottom Knuckle Type III)	Interior	Groundwater	Fast Flow, pitting
		Exterior	Groundwater	Fast Flow, pitting
	Floor Primary	Interior	Contamination Zone	Low, general
		Exterior	Grout	Anoxic
	Floor Secondary	Interior	Grout	Anoxic
		Exterior	Groundwater	Fast Flow, pitting

Table 5-12. Initial Conditions for Fast Flow Case Type IV Saturated Zone Tanks

	Location	Interior/Exterior	Environment	Mechanism
Type IV Tanks	Sidewall	Interior	Groundwater	Fast Flow, pitting
		Exterior	Groundwater	Fast Flow, pitting
	Bottom Knuckle	Interior	Groundwater	Fast Flow, pitting
		Exterior	Groundwater	Fast Flow, pitting
	Floor	Interior	Contamination Zone	Low, General
		Exterior	Groundwater	Fast Flow, pitting

Table 5-13. Initial Conditions for Fast Flow Case Type I Vadose Zone Tanks

	Location	Interior/Exterior	Environment	Mechanism
Type I Tanks	Roof Primary	Interior	Humid Air	Fast Flow, general
		Exterior	Humid Air	Fast Flow, general
	Sidewall Secondary	Interior	Humid Air	Fast Flow, general
		Exterior	Humid Air	Fast Flow, general
	Sidewall Primary	Interior	Humid Air	Fast Flow, general
		Exterior	Humid Air	Fast Flow, general
	Floor Primary	Interior	Contamination Zone	Low, general
		Exterior	Grout	Anoxic
	Floor Secondary	Interior	Contamination Zone Humid Air	Fast Flow, general
		Exterior	Concrete	Anoxic

Table 5-14. Initial Conditions for Fast Flow Case Type II Vadose Zone Tanks

	Location	Interior/Exterior	Environment	Mechanism
Type II Tanks	Roof Primary	Interior	Humid Air	Fast Flow, general
		Exterior	Humid Air	Fast Flow, general
	Sidewall Secondary	Interior	Humid Air	Fast Flow, general
		Exterior	Humid Air	Fast Flow, general
	Sidewall Primary (Top Knuckle/Top Plate)	Interior	Humid Air	Fast Flow, general
		Exterior	Humid Air	Fast Flow, general
	Sidewall Primary (Mid Plate)	Interior	Humid Air	Fast Flow, general
		Exterior	Humid Air	Fast Flow, general
	Sidewall Primary (Bottom Knuckle)	Interior	Humid Air	Fast Flow, general
		Exterior	Humid Air	Fast Flow, general
	Floor Primary	Interior	Contamination Zone	Low, general
		Exterior	Grout	Anoxic
	Floor Secondary	Interior	Contamination Zone	Low, general
		Exterior	Humid Air	Fast Flow, general

Table 5-15. Initial Conditions for Fast Flow Case Type III/IIIA Vadose Zone Tanks

	Location	Interior/Exterior	Environment	Mechanism
Type III/IIIA Tanks	Roof Secondary	Interior	Humid Air	Fast Flow, general
		Exterior	Humid Air	Fast Flow, general
	Roof Primary	Interior	Humid Air	Fast Flow, general
		Exterior	Humid Air	Fast Flow, general
	Sidewall Secondary	Interior	Humid Air	Fast Flow, general
		Exterior	Humid Air	Anoxic
	Sidewall Primary (Top Knuckle/Top Plate)	Interior	Humid Air	Fast Flow, general
		Exterior	Humid Air	Fast Flow, general
	Sidewall Primary (Mid Plate)	Interior	Humid Air	Fast Flow, general
		Exterior	Humid Air	Fast Flow, general
	Sidewall Primary (Bottom Knuckle Type IIIA)	Interior	Humid Air	Fast Flow, general
		Exterior	Humid Air	Fast Flow, general
	Sidewall Primary (Bottom Knuckle Type III)	Interior	Humid Air	Fast Flow, general
		Exterior	Humid Air	Fast Flow, general
	Floor Primary	Interior	Contamination Zone	Low, general
		Exterior	Grout	Anoxic
	Floor Secondary	Interior	Grout	Anoxic
		Exterior	Humid Air	Fast Flow, general

Table 5-16. Initial Conditions for Fast Flow Case Type IV Vadose Zone Tanks

	Location	Interior/Exterior	Environment	Mechanism
Type IV Tanks	Sidewall	Interior	Humid Air	Fast Flow, general
		Exterior	Humid Air	Fast Flow, general
	Bottom Knuckle	Interior	Humid Air	Fast Flow, general
		Exterior	Humid Air	Fast Flow, general
	Floor	Interior	Contamination Zone	Low, General
		Exterior	Humid Air	Fast Flow, general

6.0 Concrete Degradation Results

The key results from the physical evolution of concrete materials study is summarized in Table 6-1 through Table 6-3. Results for the Realistic, Compliance, and Pessimistic Cases for both the saturated and unsaturated conditions are presented. The "Limiting Time" is the time at which accelerated steel liner corrosion begins due to either 1) the arrival of a depassivating low-pH carbonation and decalcification front, or 2) environmental exposure and loss of passivation due to concrete becoming damaged by anoxic rebar corrosion, whichever occurs first. The limiting time for each tank type and component were utilized as inputs and were integrated into the steel liner corrosion model. "Damage Time" is the time at which concrete becomes completely degraded by carbonation and decalcification; these values are not used in this study but are provided for completeness.

For four of the six cases, degradation of the rebar due to anoxic corrosion resulted in the limiting time. This was true for the all the saturated zone cases and the Realistic Case vadose zone calculations. Higher gas-phase intrinsic diffusion coefficients and carbonation + dissolution rate constants, along with shorter damage front lag, resulted in shorter limiting times for the vadose zone Compliance and Pessimistic Cases. Since the concrete was assumed to be completely degraded for the Fast Flow Path Case, no limiting times were considered.

Table 6-1. Concrete Degradation for the Realistic Case

				Saturated Zone Concrete				Vadose Zone Concrete			
Tank	Component	Thickness (cm)	(in)	Carb + Decal (yr)	Damage Time (yr)	Anoxic Rebar (yr)	Limiting Time (yr)	Carb + Decal (yr)	Damage Time (yr)	Anoxic Rebar (yr)	Limiting Time (yr)
Realistic case											
Type I	Roof	55.9	22.0	31,928	34,181	11,002	11,002	31,928	34,181	11,002	11,002
Type I	Wall	55.9	22.0	31,928	34,181	10,809	10,809	31,928	34,181	10,809	10,809
Type I	Floor	76.2	30.0	43,932	46,185	9,178	9,178	43,932	46,185	9,178	9,178
Type II	Roof	114.3	45.0	66,461	68,714	21,341	21,341	66,461	68,714	21,341	21,341
Type II	Wall	83.8	33.0	48,426	50,679	16,373	16,373	48,426	50,679	16,373	16,373
Type II	Floor	106.7	42.0	61,967	64,220	22,983	22,983	61,967	64,220	22,983	22,983
Type III/IIIA	Roof	121.9	48.0	70,955	73,208	20,884	20,884	70,955	73,208	20,884	20,884
Type III/IIIA	Wall	76.2	30.0	43,932	46,185	20,393	20,393	43,932	46,185	20,393	20,393
Type III/IIIA	Floor	106.7	42.0	61,967	64,220	17,228	17,228	61,967	64,220	17,228	17,228
Type IV	Roof	17.8	7.0	9,399	11,652	4,742	4,742	9,399	11,652	1,528	1,528
Type IV	Wall	17.8	7.0	9,399	11,652	8,021	8,021	9,399	11,652	8,021	8,021
Type IV	Floor	17.5	6.9	9,222	11,474	5,418	5,418	9,222	11,474	5,418	5,418

Anoxic rebar corrosion limiting
Carbonation + Decalcification limiting

Table 6-2. Concrete Degradation for the Compliance Case

				Saturated Zone Concrete				Vadose Zone Concrete			
Tank	Component	Thickness (cm)	(in)	Carb + Decal (yr)	Damage Time (yr)	Anoxic Rebar (yr)	Limiting Time (yr)	Carb + Decal (yr)	Damage Time (yr)	Anoxic Rebar (yr)	Limiting Time (yr)
Compliance case											
Type I	Roof	55.9	22.0	31,928	34,181	11,002	11,002	2,658	2,845	11,002	2,658
Type I	Wall	55.9	22.0	31,928	34,181	10,809	10,809	2,658	2,845	10,809	2,658
Type I	Floor	76.2	30.0	43,932	46,185	9,178	9,178	3,657	3,844	9,178	3,657
Type II	Roof	114.3	45.0	66,461	68,714	21,341	21,341	5,532	5,720	21,341	5,532
Type II	Wall	83.8	33.0	48,426	50,679	16,373	16,373	4,031	4,218	16,373	4,031
Type II	Floor	106.7	42.0	61,967	64,220	22,983	22,983	5,158	5,346	22,983	5,158
Type III/IIIA	Roof	121.9	48.0	70,955	73,208	20,884	20,884	5,906	6,094	20,884	5,906
Type III/IIIA	Wall	76.2	30.0	43,932	46,185	20,393	20,393	3,657	3,844	20,393	3,657
Type III/IIIA	Floor	106.7	42.0	61,967	64,220	17,228	17,228	5,158	5,346	17,228	5,158
Type IV	Roof	17.8	7.0	9,399	11,652	4,742	4,742	782	970	4,742	782
Type IV	Wall	17.8	7.0	9,399	11,652	8,021	8,021	782	970	8,021	782
Type IV	Floor	17.5	6.9	9,222	11,474	5,418	5,418	768	955	5,418	768

Anoxic rebar corrosion limiting
Carbonation + Decalcification limiting

Table 6-3. Concrete Degradation for Pessimistic Case

				Saturated Zone Concrete				Vadose Zone Concrete			
Tank	Component	Thickness (cm)	(in)	Carb + Decal (yr)	Damage Time (yr)	Anoxic Rebar (yr)	Limiting Time (yr)	Carb + Decal (yr)	Damage Time (yr)	Anoxic Rebar (yr)	Limiting Time (yr)
Pessimistic case											
Type I	Roof	55.9	22.0	21,536	22,537	11,002	11,002	755	790	11,002	755
Type I	Wall	55.9	22.0	21,536	22,537	10,809	10,809	755	790	10,809	755
Type I	Floor	76.2	30.0	9,846	10,180	9,178	9,178	345	357	9,178	345
Type II	Roof	114.3	45.0	44,558	45,559	21,341	21,341	1,562	1,597	21,341	1,562
Type II	Wall	83.8	33.0	32,534	33,535	16,373	16,373	1,140	1,175	16,373	1,140
Type II	Floor	106.7	42.0	13,854	14,188	22,983	13,854	486	497	22,983	486
Type III/IIIA	Roof	121.9	48.0	47,554	48,555	20,884	20,884	1,667	1,702	20,884	1,667
Type III/IIIA	Wall	76.2	30.0	29,538	30,539	20,393	20,393	1,035	1,070	20,393	1,035
Type III/IIIA	Floor	106.7	42.0	13,854	14,188	17,228	13,854	486	497	17,228	486
Type IV	Roof	17.8	7.0	6,516	7,518	4,742	4,742	228	263	4,742	228
Type IV	Wall	17.8	7.0	6,516	7,518	8,021	6,516	228	263	8,021	228
Type IV	Floor	17.5	6.9	2,133	2,466	5,418	2,133	75	86	5,418	75

Anoxic rebar corrosion limiting
Carbonation + Decalcification limiting

7.0 Approach to Calculations

The calculations demonstrate how the steel degradation progresses with time for each scenario. The relationship between the degradation and failure of the concrete is also illustrated. The objective of these calculations was to determine the minimum failure time for a given plate location in each tank type for each scenario. A decision logic diagram was developed to show how these calculations were connected. Before describing the diagram, variables presented in the diagram are described.

t_{if}:	total time until the wall thickness is penetrated given the corrosion rate for the initial condition
t_L:	total time to complete degradation of concrete or limiting time, see concrete degradation tables in Section 6.0
t_a:	time when accelerated corrosion is initiated, or carb + decal time from concrete degradation tables in Section 6.0
t_{af}:	total time until the wall thickness is penetrated given the corrosion rate for the initial condition by accelerated condition
t_{ff}:	total time until the wall thickness is penetrated by fast flow path mechanism

The decision logic diagram is presented in Figure 7-1 through Figure 7-3. The diagram in Figure 7-1 determines whether or not a plate of steel degrades completely by corrosion in the initial environment prior to degradation of the concrete or after the initiation of an accelerated corrosion mechanism (e.g., carbonation). If the concrete degrades completely prior to failure in the initial environment or the Fast Flow Path Case is being considered, the calculations were continued in Figure 7-3. On the other hand, if an accelerated mechanism (e.g., carbonation) is initiated prior to failure of the plate of steel, the calculations were continued in Figure 7-2.

Figure 7-2 determines the time for degradation by an accelerated corrosion mechanism. If the concrete degrades completely before the steel plate is penetrated by the accelerated mechanism, the calculations were continued in Figure 7-3. In Figure 7-3, the time to failure of the steel by the Fast Flow Path Case was determined.

The steel liner progression model has two key aspects. First, the model assumes an immediate transition between corrosion mechanism (e.g., anoxic, passive corrosion transitions to carbonation induced corrosion upon the arrival of the carbonation front). While this transition is not likely to occur immediately due to the presence of iron oxides, it may be expected that the transition occurs gradually over a period that is relatively short in comparison to the failure

times. Secondly, the exterior and interior sides of a plate may experience different environments at the same time and thus different corrosion rates. Thus, the total corrosion rate for the plate is simply the sum of the two corrosion rates (e.g., anoxic, passive corrosion occurs at 0.04 mpy and indoor air corrosion occurs at 0.4 mpy, thus the total corrosion rate on a secondary wall plate would be 0.44 mpy).

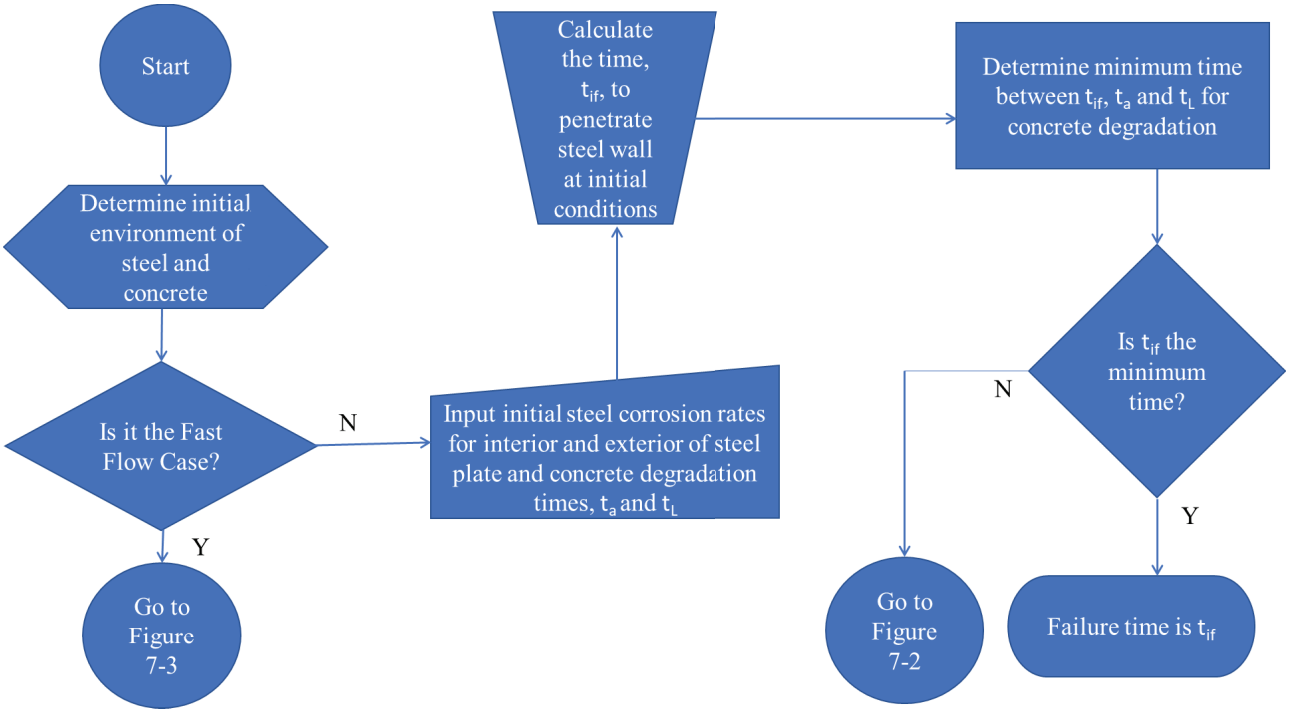

Figure 7-1. Decision Tree Logic for Initial Mechanism Failure

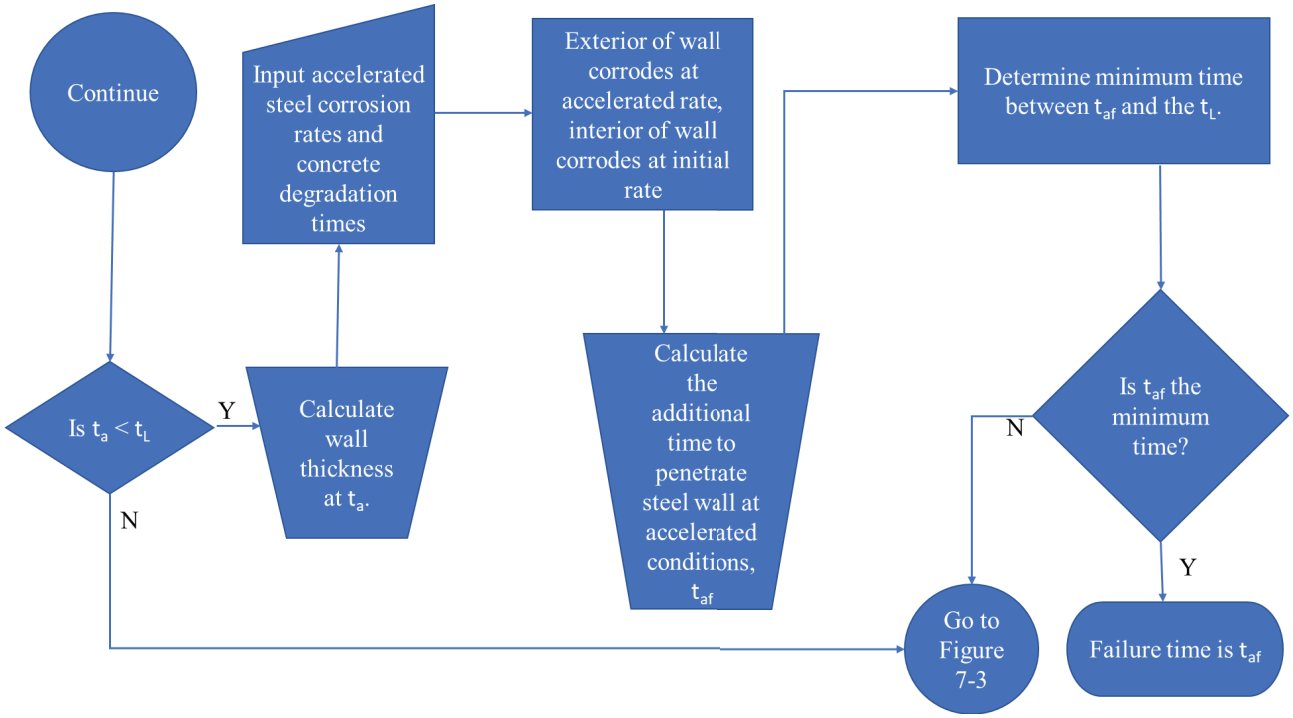

Figure 7-2. Decision Tree Logic for Accelerated Mechanism Failure

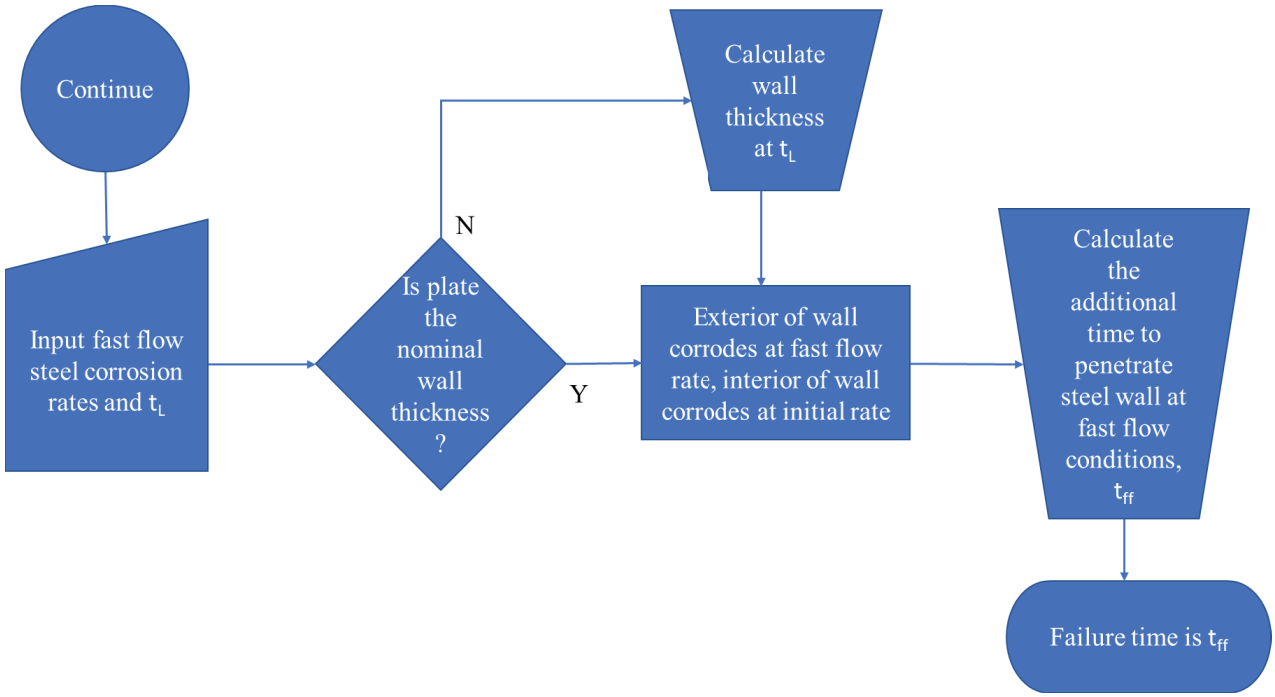

Figure 7-3. Decision Tree Logic for Fast Flow Path Mechanism Failure

8.0 Steel Component Degradation Results

The estimated life of the steel components was considered for the four cases: Realistic, Compliance, Pessimistic, and Fast Flow Path. The steel components considered were the plates of steel that comprise the primary tank, the plates of steel that comprise the secondary tank, and the internal cooling coil piping for the Type I, II, and III/IIIA tanks.

8.1 Realistic Case

8.1.1 Saturated Zone

The failure times and mechanisms for the steel plates in each tank type and location are shown in Table 8-1. In most cases, the failure occurred due to anoxic, passive corrosion in the concrete/grout environment. In this situation, both the interior and exterior sides of a plate of steel corroded at 0.04 mpy. Figure 8-1 also shows the time the steel at each of these locations in a Type III/IIIA tank will fail. There are three exceptions shown in Table 8-1: the floor of the secondary and primary tank for the Type I tank and the floor of the Type IV tank. In these cases, the concrete degraded due to failure of the rebar, and thus did not meet the minimum diameter criteria for structural stability in year 2484. The rebar had corroded by anoxic, passive corrosion. Once the concrete had degraded, the exterior of the floor was exposed to a groundwater environment. This evolution is shown in Figure 8-2. The floor of the liner achieved 25% breach within 11 years after the concrete had degraded. This evolution illustrates how the degradation of the concrete and the corrosion of the steel are coupled in this approach.

For this case, it was assumed that the cooling coils and the interior of the tank were grouted such that no air gaps existed between the steel and the grout. Thus, anoxic passive corrosion occurred on both sides of the pipe wall. Given that the wall thickness for all the cooling coils is 0.154 inches (2 inch, Schedule 40 pipe), the estimated life of the cooling coils before they are penetrated is 1925 years (Table 8-1).

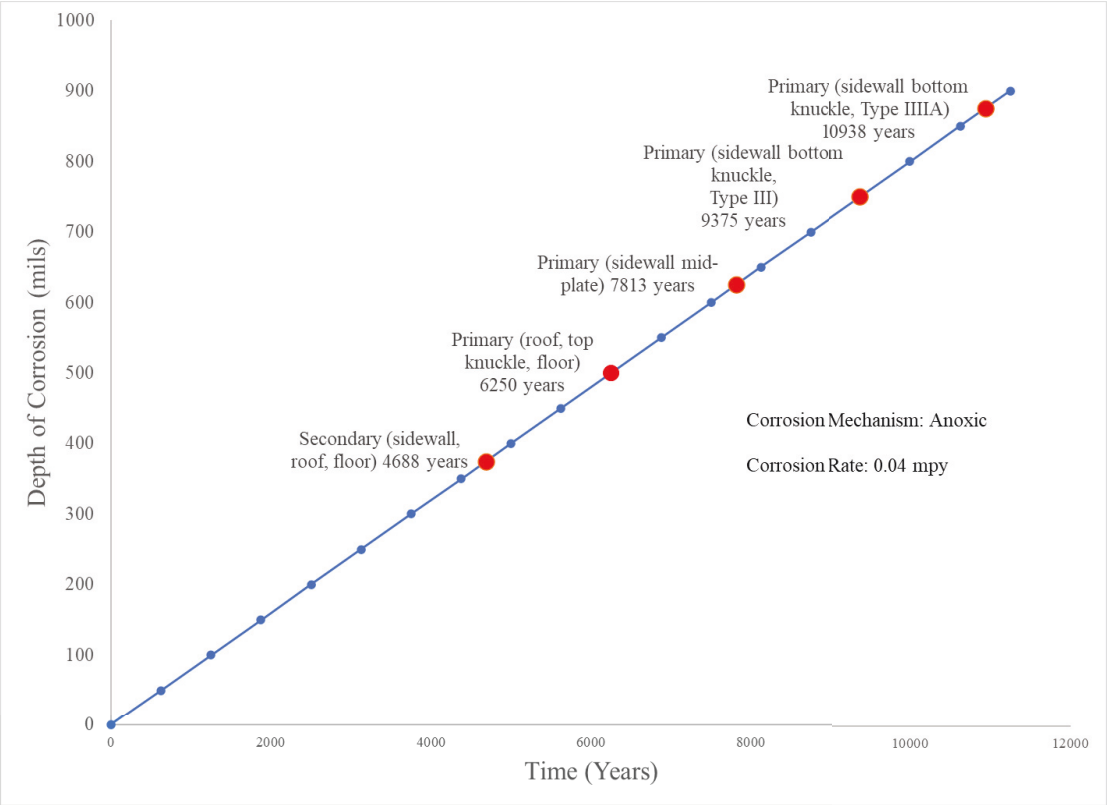

Figure 8-1. Failure of Type III/IIIA Tank for Realistic Case

Table 8-1. Failure Times for the Saturated Zone, Realistic Case

		Time (yrs)	Mechanism
Type I Tanks	Roof Primary	6250	Anoxic
	Sidewall Secondary	6250	Anoxic
	Sidewall Primary	6250	Anoxic
	Floor Primary	3941	Anoxic/Groundwater
	Floor Secondary	3929	Anoxic/Groundwater
	Cooling Coils	1925	Anoxic
Type II Tanks	Roof Primary	6250	Anoxic
	Sidewall Secondary	6250	Anoxic
	Sidewall Primary (Top Knuckle/Top Plate)	7038	Anoxic
	Sidewall Primary (Mid Plate)	7813	Anoxic
	Sidewall Primary (Bottom Knuckle)	10938	Anoxic
	Floor Primary	6250	Anoxic
	Floor Secondary	6250	Anoxic
	Cooling Coils	1925	Anoxic
Type III/IIIA Tanks	Roof Secondary	4688	Anoxic
	Roof Primary	6250	Anoxic
	Sidewall Secondary	4688	Anoxic
	Sidewall Primary (Top Knuckle/Top Plate)	6250	Anoxic
	Sidewall Primary (Mid Plate)	7813	Anoxic
	Sidewall Primary (Bottom Knuckle Type IIIA)	10938	Anoxic
	Sidewall Primary (Bottom Knuckle Type III)	9375	Anoxic
	Floor Primary	6250	Anoxic
	Floor Secondary	4688	Anoxic
	Cooling Coils	1925	Anoxic
Type IV Tanks	Sidewall	4688	Anoxic
	Bottom Knuckle	5469	Anoxic
	Floor	2495	Anoxic/Groundwater

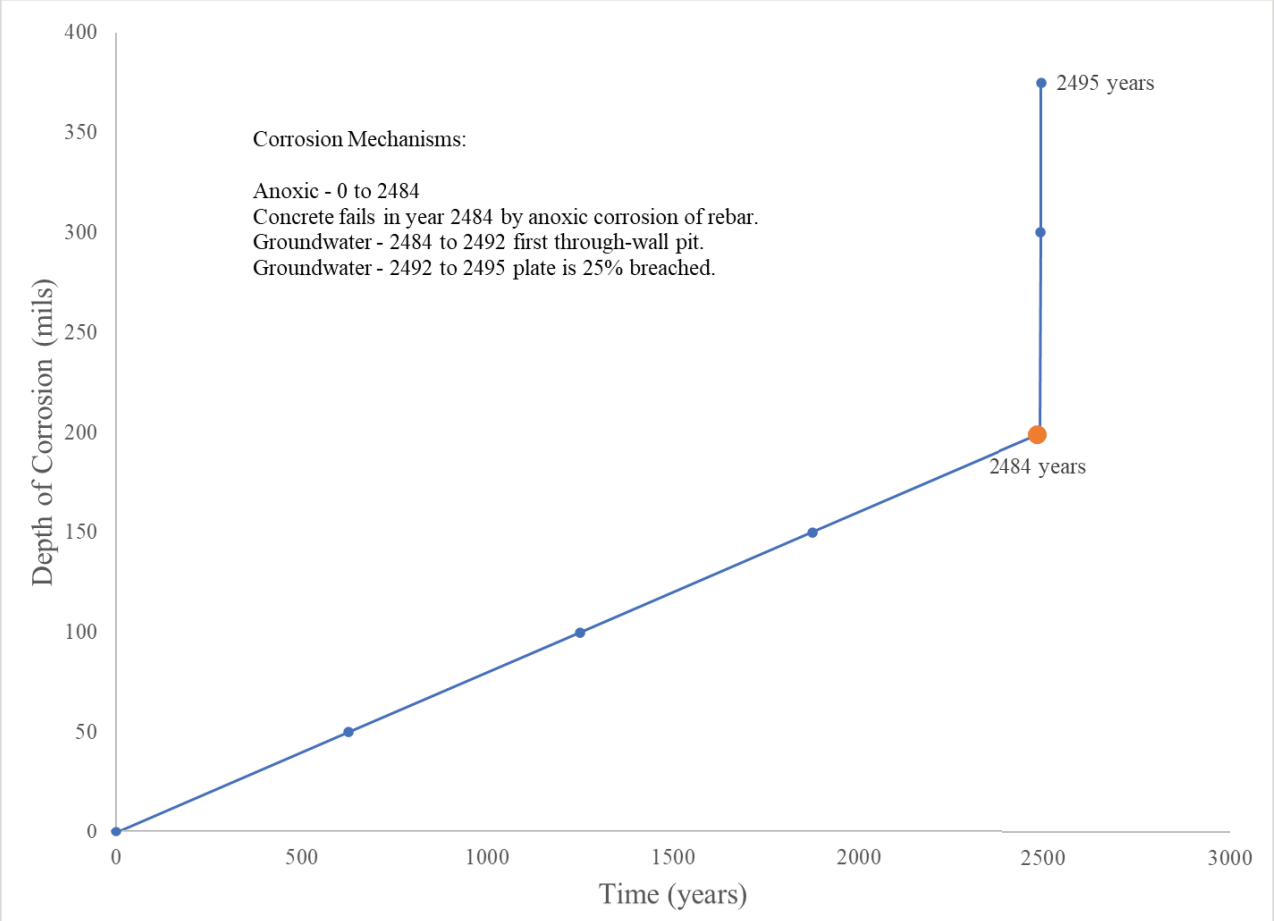

Figure 8-2. Failure of Type IV Tank for the Saturated Zone, Realistic Case

8.1.2 Vadose Zone

The failure times and mechanisms for the steel plates in each tank type and location are shown in Table 8-2. In most cases, the failure occurred due to anoxic, passive corrosion in the concrete/grout environment similar to the saturated zone case. In this situation, both the interior and exterior sides of a plate of steel corroded at 0.04 mpy. There are three exceptions noted: the floor of the secondary and primary tank for the Type I tank and the floor of the Type IV tank. As with the saturated zone case, the concrete degraded due to failure of the rebar, and thus did not meet the minimum diameter criteria for structural stability in year 3918. The rebar had corroded by anoxic, passive corrosion. Once the concrete had degraded, the exterior of the secondary floor was exposed to a humid environment. The corrosion rate of the exterior secondary floor accelerated to the value for humid air, while the interior floor corroded at the anoxic, passive corrosion rate. The general corrosion rate was taken to be the sum of these two corrosion rates or 2.07 mpy. The floor of the primary wall continued to corrode at the anoxic, passive corrosion rate until the floor of the secondary was penetrated at year 4008, for the Type I tank. At this

stage the exterior floor of the primary was assumed to be under humid air conditions, and the rate of corrosion for the whole plate accelerated to 2.07 mpy. This evolution is shown in Figure 8-3. The primary floor was penetrated by year 4095, which is about 90 years after exposure to the humid air. Clearly the groundwater is a more corrosive condition than humid air once the environment contacts the steel.

For this case, it was assumed that the cooling coils and the interior of the tank were grouted such that no air gaps existed between the steel and the grout. Thus, anoxic passive corrosion occurred on both sides of the pipe wall. Given that the wall thickness for all the cooling coils is 0.154 inches (2 inch, Schedule 40 pipe), the estimated life of the cooling coils before they are penetrated is 1925 years (Table 8-2).

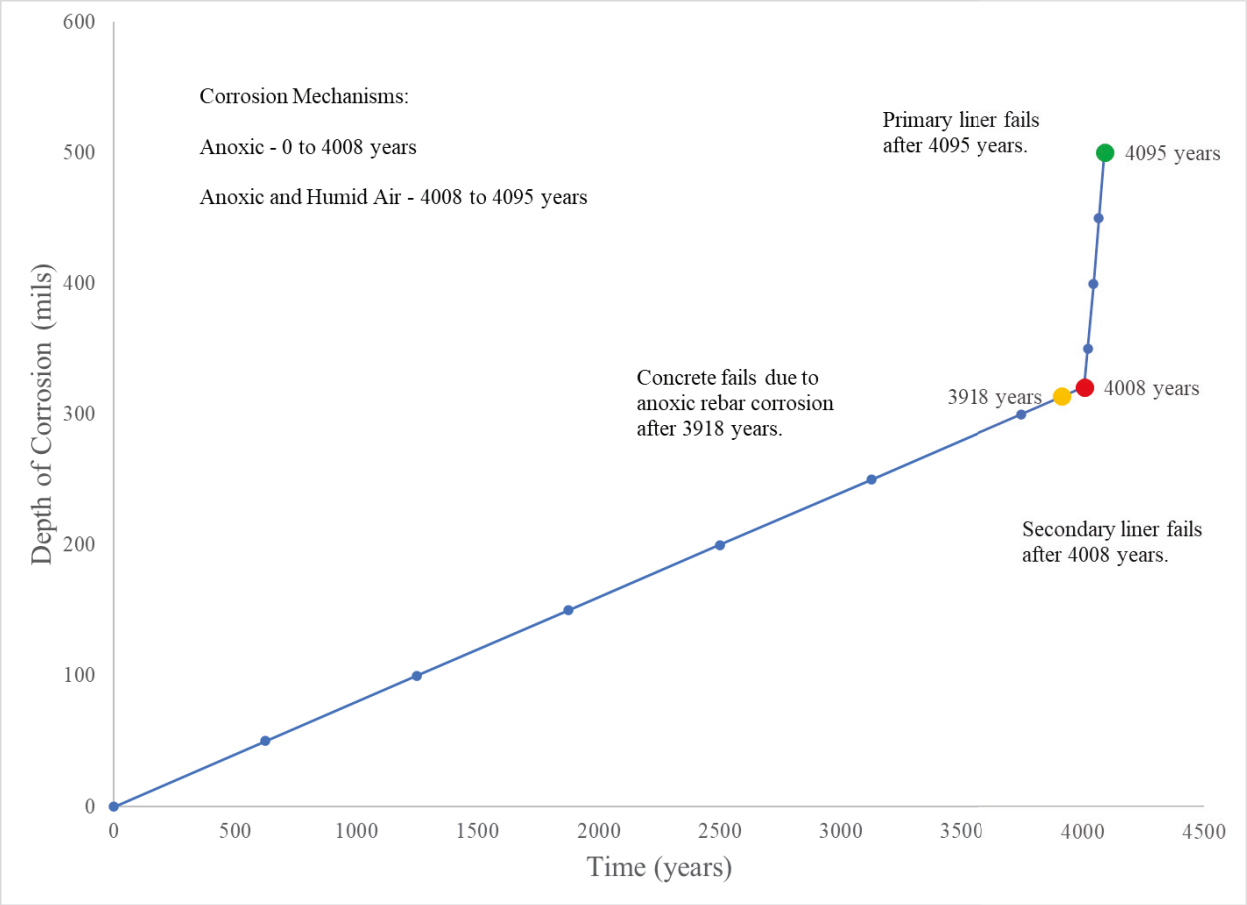

Figure 8-3 Failure of Type IV Tank for the Vadose Zone, Realistic Case

Table 8-2. Failure Times for the Vadose Zone, Realistic Case

		Time (yrs)	Mechanism
Type I Tanks	Roof Primary	6250	Anoxic
	Sidewall Secondary	6250	Anoxic
	Sidewall Primary	6250	Anoxic
	Floor Primary	4095	Anoxic/Humid Air
	Floor Secondary	4008	Anoxic/Humid Air
	Cooling Coils	1925	Anoxic
Type II Tanks	Roof Primary	6250	Anoxic
	Sidewall Secondary	6250	Anoxic
	Sidewall Primary (Top Knuckle/Top Plate)	7038	Anoxic
	Sidewall Primary (Mid Plate)	7813	Anoxic
	Sidewall Primary (Bottom Knuckle)	10938	Anoxic
	Floor Primary	6250	Anoxic
	Floor Secondary	6250	Anoxic
	Cooling Coils	1925	Anoxic
Type III/IIIA Tanks	Roof Secondary	4688	Anoxic
	Roof Primary	6250	Anoxic
	Sidewall Secondary	4688	Anoxic
	Sidewall Primary (Top Knuckle/Top Plate)	6250	Anoxic
	Sidewall Primary (Mid Plate)	7813	Anoxic
	Sidewall Primary (Bottom Knuckle Type IIIA)	10938	Anoxic
	Sidewall Primary (Bottom Knuckle Type III)	9375	Anoxic
	Floor Primary	6250	Anoxic
	Floor Secondary	6250	Anoxic
	Cooling Coils	1925	Anoxic
Type IV Tanks	Sidewall	4688	Anoxic
	Bottom Knuckle	5469	Anoxic
	Floor	2569	Anoxic/Humid Air

8.2 Compliance Case

8.2.1 Saturated Zone

The failure times and mechanisms for the steel plates in each tank type and location are shown in Table 8-3. In most cases, the failure occurred due to anoxic, passive corrosion in the concrete/grout environment. In this situation, both the interior and exterior sides of a plate of steel corroded at 0.04 mpy. Figure 8-1 also shows the time the steel at each of these locations in a Type III/IIIA tank will fail. There are three exceptions shown in Table 8-3: the floor of the secondary and primary tank for the Type I tank and the floor of the Type IV tank. In this case, the concrete degraded due to failure of the rebar, and thus did not meet the minimum diameter criteria for structural stability in year 2484. The rebar had corroded by anoxic, passive corrosion. Once the concrete had degraded, the exterior of the floor was exposed to a groundwater environment. The floor of the liner achieved 25% breach within 11 years after the concrete had degraded.

This evolution illustrates how the degradation of the concrete and the corrosion of the steel are coupled in this approach. These results were the same as those for the saturated zone, Realistic Case. This was expected given the diffusion coefficient for carbonation, the corrosion rate of the rebar, and the damage front lag did not change for the two cases.

For this case, it was assumed that the exterior of the cooling coils was grouted such that no air gaps existed between the steel and the grout. However, the cooling coils were not adequately grouted. Thus, anoxic passive corrosion occurred on the exterior of the pipe, while indoor air corrosion occurred on the interior. Given that the wall thickness for all the cooling coils is 0.154 inches (2 inch, Schedule 40 pipe), the estimated life of the cooling coils before they are penetrated is 350 years (Table 8-3).

Table 8-3. Failure Times for the Saturated Zone, Compliance Case

		Time (yrs)	Mechanism
Type I Tanks	Roof Primary	6250	Anoxic
	Sidewall Secondary	6250	Anoxic
	Sidewall Primary	6250	Anoxic
	Floor Primary	3941	Anoxic/Groundwater
	Floor Secondary	3929	Anoxic/Groundwater
	Cooling Coils	350	Anoxic/Indoor Air
Type II Tanks	Roof Primary	6250	Anoxic
	Sidewall Secondary	6250	Anoxic
	Sidewall Primary (Top Knuckle/Top Plate)	7038	Anoxic
	Sidewall Primary (Mid Plate)	7813	Anoxic
	Sidewall Primary (Bottom Knuckle)	10938	Anoxic
	Floor Primary	6250	Anoxic
	Floor Secondary	6250	Anoxic
	Cooling Coils	350	Anoxic/Indoor Air
Type III/IIIA Tanks	Roof Secondary	4688	Anoxic
	Roof Primary	6250	Anoxic
	Sidewall Secondary	4688	Anoxic
	Sidewall Primary (Top Knuckle/Top Plate)	6250	Anoxic
	Sidewall Primary (Mid Plate)	7813	Anoxic
	Sidewall Primary (Bottom Knuckle Type IIIA)	10938	Anoxic
	Sidewall Primary (Bottom Knuckle Type III)	9375	Anoxic
	Floor Primary	6250	Anoxic
	Floor Secondary	4688	Anoxic
	Cooling Coils	350	Anoxic/Indoor Air
Type IV Tanks	Sidewall	4688	Anoxic
	Bottom Knuckle	5469	Anoxic
	Floor	2495	Anoxic/Groundwater

8.2.2 Vadose Zone

The failure times and mechanisms for the steel plates in each tank type and location are shown in Table 8-4. In most cases, the failure occurred due to a sequence of corrosion mechanisms. The most common sequence was 1) anoxic, passive corrosion, 2) carbonation, and 3) humid air. This sequence occurred on all but the primary tank sidewall. Figure 8-4, which is for the sidewall secondary location of a Type III/IIIA tank, illustrates this progression. In this situation, both the interior and exterior sides of a plate of steel initially corroded at 0.04 mpy. The carbonation front arrived at the exterior of the secondary wall in year 3657 and the corrosion rate accelerated to 0.27 mpy. Before the secondary wall is penetrated, the concrete sidewall fails due to anoxic corrosion of the rebar in year 3844. The plate was now exposed to humid air on the exterior side and the corrosion rate accelerated to 2.07 mpy. Thus, failure occurred due to humid air on the exterior and anoxic, passive corrosion the interior in year 3860.

The primary sidewall was afforded more protection because of a 30-inch layer of grout that exists in the annulus between the secondary and primary wall. In this case the carbonation layer does not reach the exterior of the top plate of the primary wall before it is penetrated by anoxic, passive corrosion. The remaining plates of the primary wall are thick enough such that the carbonation front reaches the exterior wall before it is penetrated.

The final variant is seen in how the roof and floor are penetrated. In both situations, the secondary steel is penetrated by anoxic, passive corrosion. However, afterwards before the primary can corrode in the same manner, the rebar corrodes such that the minimum diameter requirement is not met and thus the concrete degrades. Thus, the exterior of the primary is exposed to humid air just before the wall is penetrated. These examples again show how the degradation of the steel and concrete are coupled together.

For this case, it was assumed that the exterior of the cooling coils was grouted such that no air gaps existed between the steel and the grout. However, the cooling coils were not adequately grouted. Thus, anoxic passive corrosion occurred on the exterior of the pipe, while indoor air corrosion occurred on the interior. Given that the wall thickness for all the cooling coils is 0.154 inches (2 inch, Schedule 40 pipe), the estimated life of the cooling coils before they are penetrated is 350 years (Table 8-4).

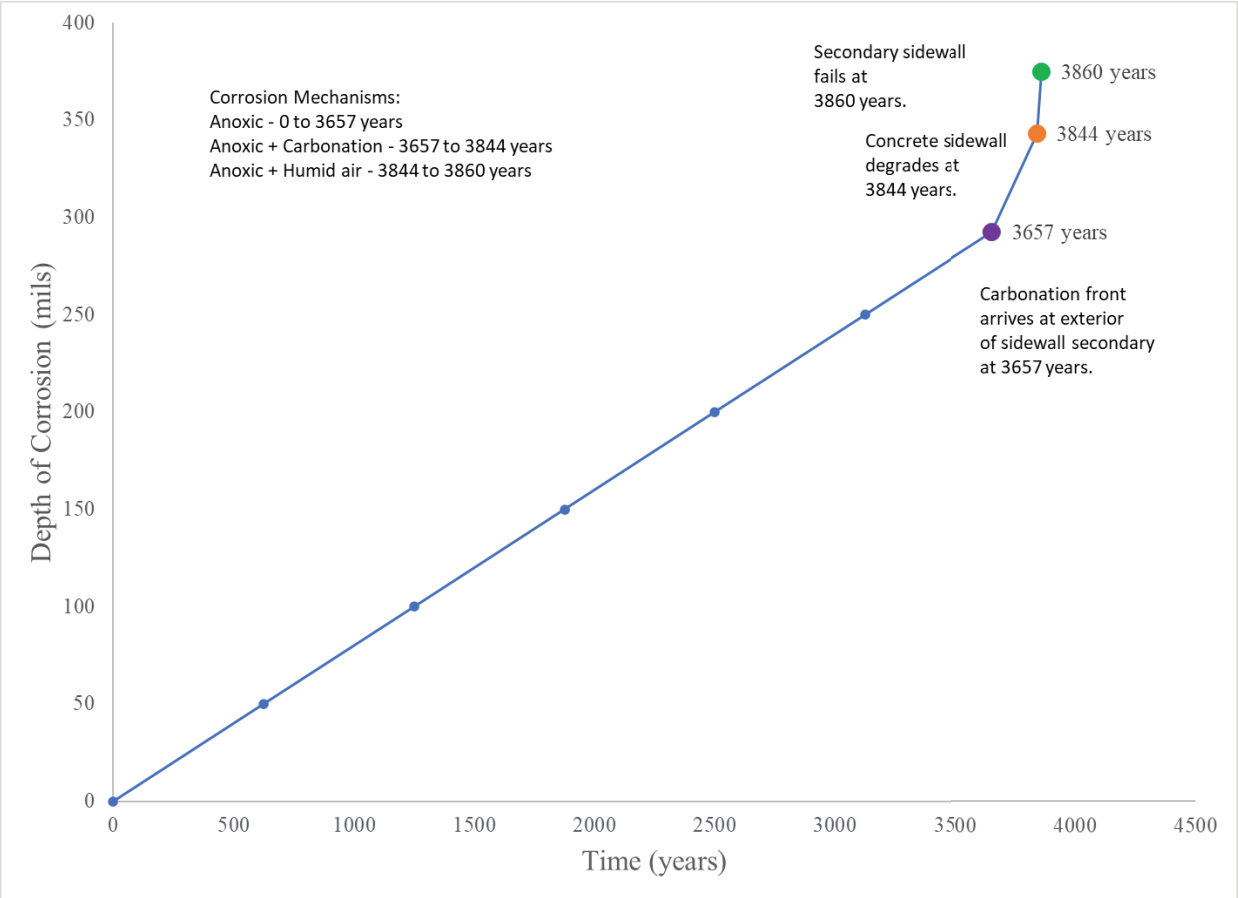

Figure 8-4. Failure of Type IV Tank for the Vadose Zone, Compliance Case

Table 8-4. Failure Times for the Vadose Zone, Compliance Case

		Time (yrs)	Mechanism
Type I Tanks	Roof Primary	2960	Anoxic/Carbonation/Humid Air
	Sidewall Secondary	2960	Anoxic/Carbonation/Humid Air
	Sidewall Primary	6250	Anoxic
	Floor Primary	4010	Anoxic/Carbonation/Humid Air
	Floor Secondary	3920	Anoxic/Carbonation/Humid Air
	Cooling Coils	350	Anoxic/Indoor Air
Type II Tanks	Roof Primary	5723	Anoxic/Carbonation/Humid Air
	Sidewall Secondary	4280	Anoxic/Carbonation/Humid Air
	Sidewall Primary (Top Knuckle/Top Plate)	7038	Anoxic
	Sidewall Primary (Mid Plate)	7793	Anoxic/Carbonation
	Sidewall Primary (Bottom Knuckle)	8719	Anoxic/Carbonation
	Floor Primary	5516	Anoxic/Humid Air
	Floor Secondary	5363	Anoxic/Carbonation/Humid Air
	Cooling Coils	350	Anoxic/Indoor Air
Type III/IIIA Tanks	Roof Secondary	4688	Anoxic
	Roof Primary	6100	Anoxic/Humid Air
	Sidewall Secondary	3860	Anoxic/Carbonation/Humid Air
	Sidewall Primary (Top Knuckle/Top Plate)	6250	Anoxic
	Sidewall Primary (Mid Plate)	6826	Anoxic/Carbonation
	Sidewall Primary (Bottom Knuckle Type IIIA)	7751	Anoxic/Carbonation
	Sidewall Primary (Bottom Knuckle Type III)	7289	Anoxic/Carbonation
	Floor Primary	5381	Anoxic/Humid Air
	Floor Secondary	4688	Anoxic
	Cooling Coils	350	Anoxic/Indoor Air
Type IV Tanks	Sidewall	1096	Anoxic/Carbonation/Humid Air
	Bottom Knuckle	1127	Anoxic/Carbonation/Humid Air
	Floor	1082	Anoxic/Carbonation/Humid Air

8.3 Pessimistic Case

8.3.1 Saturated Zone

The failure times and mechanisms for the steel plates in each tank type and location are shown in Table 8-5. In this case gaps between the grout and steel walls due to shrinkage create a condition where corrosion may be accelerated by indoor air. Failure times ranged between 625 to 1136 years for all but the floor locations, which is approximately a factor of 5 reduction compared to previous scenarios. Since no gaps were assumed for the floor, the failure occurred due to anoxic, passive corrosion in the concrete/grout environment.

Figure 8-5 compares the time to penetrate the Type III tank secondary roof due to anoxic corrosion versus indoor air. The order of magnitude increase in the corrosion rate of the steel on the interior reduces the time to penetration of the roof by a factor of five. The floor for each type of tank does not corrode as rapidly since it is assumed that gaps between the grout and the floor do not exist. The floor still fails due to attack by the groundwater because the concrete degrades to the anoxic corrosion of the rebar.

For this case, it was assumed that the exterior of the cooling coils was grouted such that no air gaps existed between the steel and the grout. However, the cooling coils were not adequately grouted. Thus, anoxic passive corrosion occurred on the exterior of the pipe, while indoor air corrosion occurred on the interior. Given that the wall thickness for all the cooling coils is 0.154 inches (2 inch, Schedule 40 pipe), the estimated life of the cooling coils before they are penetrated is 350 years (Table 8-5).

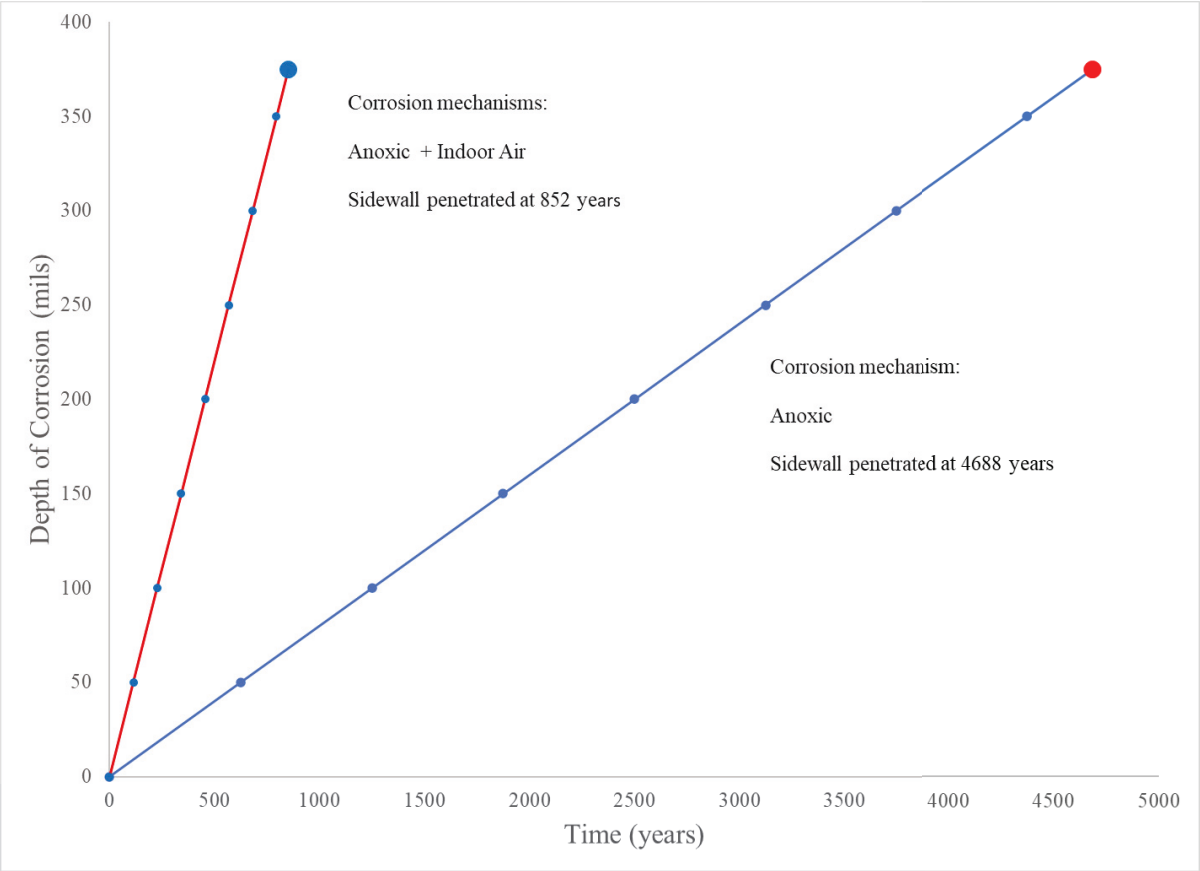

Figure 8-5. Failure of Type III/IIIA Tank for the Saturated Zone, Pessimistic Case

Table 8-5. Failure Times for the Saturated Zone, Pessimistic Case

		Time (yrs)	Mechanism
Type I Tanks	Roof Primary	1136	Anoxic/Indoor Air
	Sidewall Secondary	1136	Anoxic/Indoor Air
	Sidewall Primary	625	Indoor Air
	Floor Primary	3941	Anoxic/Groundwater
	Floor Secondary	3929	Anoxic/Groundwater
	Cooling Coils	350	Anoxic/Indoor Air
Type II Tanks	Roof Primary	1136	Anoxic/Indoor Air
	Sidewall Secondary	1136	Anoxic/Indoor Air
	Sidewall Primary (Top Knuckle/Top Plate)	704	Indoor Air
	Sidewall Primary (Mid Plate)	781	Indoor Air
	Sidewall Primary (Bottom Knuckle)	1094	Indoor Air
	Floor Primary	6250	Anoxic
	Floor Secondary	6250	Anoxic
	Cooling Coils	350	Anoxic/Indoor Air
Type III/IIIA Tanks	Roof Secondary	852	Anoxic/Indoor Air
	Roof Primary	625	Indoor Air
	Sidewall Secondary	852	Anoxic/Indoor Air
	Sidewall Primary (Top Knuckle/Top Plate)	625	Indoor Air
	Sidewall Primary (Mid Plate)	781	Indoor Air
	Sidewall Primary (Bottom Knuckle Type III)	938	Indoor Air
	Sidewall Primary (Bottom Knuckle Type IIIA)	1094	Indoor Air
	Floor Primary	6250	Anoxic
	Floor Secondary	6250	Anoxic
	Cooling Coils	350	Anoxic/Indoor Air
Type IV Tanks	Sidewall	852	Anoxic/Indoor Air
	Bottom Knuckle	994	Anoxic/Indoor Air
	Floor	2477	Anoxic/Groundwater

8.3.2 Vadose Zone

The failure times and mechanisms for the steel plates in each tank type and location are shown in Table 8-6. Due to shrinkage of the grout, indoor air is the predominant mechanism prior to complete degradation of the concrete. In fact, it is the only failure mechanism for the primary sidewall for the Type I, II and III tanks. Because the concrete vault wall is thinner for the Type IV tanks, carbonation initiates corrosion on the exterior secondary wall and causes complete degradation of the concrete, which allows humid air corrosion to fully penetrate the sidewall.

The secondary roof and sidewall may fail by a combination of anoxic, passive corrosion and indoor air provided the wall is thick enough (e.g., see Type II and III/IIIA tanks). For thinner concrete walls, such as the roof of the Type I tanks, the carbonation front reaches the exterior of the roof and results in degradation of the concrete prior to penetration. Thus, humid air corrosion also occurs for the roof of the Type I tanks.

Finally, failure calculations for the floor illustrates the effect of assuming the presence of structural cracks in the horizontal beam. It was assumed that the floor had structural cracks present on the exterior of the concrete vault, and thus the diffusion coefficient was three times greater than a beam with no cracks (e.g., the sidewall). The effect can be demonstrated by comparing the time to failure for the Type IV tank sidewall and the Type IV tank floor (see Figure 8-6). The wall thickness for the sidewall and the floor are the same, 0.375 inches. Initially the sidewall corrodes at a faster rate because the interior is exposed to indoor air, while the floor is exposed only to anoxic, passive corrosion. However, the carbonation front reaches the exterior of the floor much sooner than the sidewall (75 years vs. 228 years). The concrete floor completely degrades within 11 years and exposes the floor to the humid air condition, which accelerates corrosion significantly. Thus, the floor is predicted to fail in 263 years, while the sidewall fails in 367 years. This same effect is also seen when comparing the sidewall secondary and the floor secondary for the Type I, II, and III/IIIA tanks.

For this case, it was assumed that the exterior of the cooling coils was grouted such that no air gaps existed between the steel and the grout. However, the cooling coils were not adequately grouted. Thus, anoxic passive corrosion occurred on the exterior of the pipe, while indoor air corrosion occurred on the interior. Given that the wall thickness for all the cooling coils is 0.154 inches (2 inch, Schedule 40 pipe), the estimated life of the cooling coils before they are penetrated is 350 years (Table 8-6).

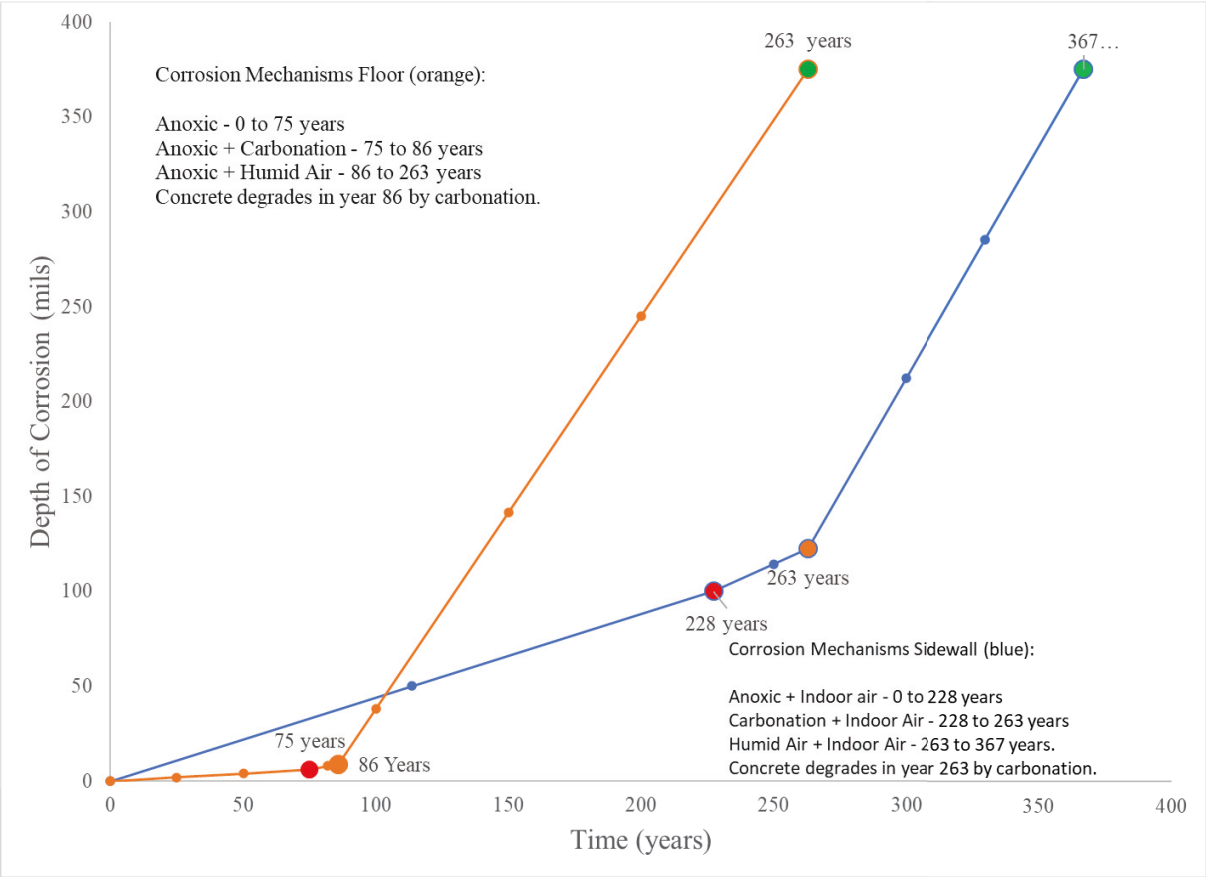

Figure 8-6. Failure of Type IV Tank for the Vadose Zone, Pessimistic Case

Table 8-6. Failure Times for the Vadose Zone, Pessimistic Case

		Time (yrs)	Mechanism
Type I Tanks	Roof Primary	850	Indoor Air/Anoxic/Carbonation/Humid Air
	Sidewall Secondary	850	Indoor Air/Anoxic/Carbonation/Humid Air
	Sidewall Primary	625	Indoor Air
	Floor Primary	802	Anoxic/Humid Air
	Floor Secondary	583	Anoxic/Carbonation/Humid Air
	Cooling Coils	350	Anoxic/Indoor Air
Type II Tanks	Roof Primary	1136	Anoxic/Indoor Air
	Sidewall Secondary	1136	Anoxic/Indoor Air
	Sidewall Primary (Top Knuckle/Top Plate)	704	Indoor Air
	Sidewall Primary (Mid Plate)	781	Indoor Air
	Sidewall Primary (Bottom Knuckle)	1094	Indoor Air
	Floor Primary	932	Anoxic/Humid Air
	Floor Secondary	718	Anoxic/Carbonation/Humid Air
	Cooling Coils	350	Anoxic/Indoor Air
Type III/IIIA Tanks	Roof Secondary	852	Anoxic/Indoor Air
	Roof Primary	625	Indoor Air
	Sidewall Secondary	852	Anoxic/Indoor Air
	Sidewall Primary (Top Knuckle/Top Plate)	625	Indoor Air
	Sidewall Primary (Mid Plate)	781	Indoor Air
	Sidewall Primary (Bottom Knuckle Type IIIA)	1078	Indoor Air/Humid Air
	Sidewall Primary (Bottom Knuckle Type III)	938	Indoor Air
	Floor Primary	874	Anoxic/Humid Air
	Floor Secondary	658	Anoxic/Carbonation/Humid Air
	Cooling Coils	350	Anoxic/Indoor Air
Type IV Tanks	Sidewall	367	Anoxic/Indoor Air/Humid Air
	Bottom Knuckle	393	Anoxic/Indoor Air/Humid Air
	Floor	263	Anoxic/Carbonation/Humid Air

8.4 Fast Flow Path Case

8.4.1 Saturated Zone

This calculation shows the effect of direct exposure of the steel plates to a corrosive groundwater environment. The results are summarized in Table 8-7. The concrete and grout provide essentially no protection, except that initially it was assumed that there was no grout shrinkage next to the floors. Thus, anoxic, passive corrosion could occur in these areas. However, because the groundwater is very corrosive, the failure times are very short. Once pitting corrosion due to the groundwater commenced, the failure times were typically within 10-20 years. The evolution of the steel liner failure is shown in Figure 8-7.

The failure times of the steel wall were compared to those for carbon transfer line jackets in F-Area [68]. These lines were exposed to saturated soil and failed by pitting corrosion. The 0.25-inch lines were breached after approximately 25 years of service. Thus, the assumed groundwater pitting corrosion rate is high, but within a factor of 2-3 of the rate observed on the carbon steel pipe. A marginal change would be observed by assuming the more recent site data.

For this case, it was assumed that both the interior and exterior of the cooling coils were not adequately grouted and that the concrete had degraded. Thus, humid air corrosion occurred on both sides of the pipe wall. Given that the wall thickness for all the cooling coils is 0.154 inches (2 inch, Schedule 40 pipe), the estimated life of the cooling coils before they are penetrated is 38 years (Table 8-7).

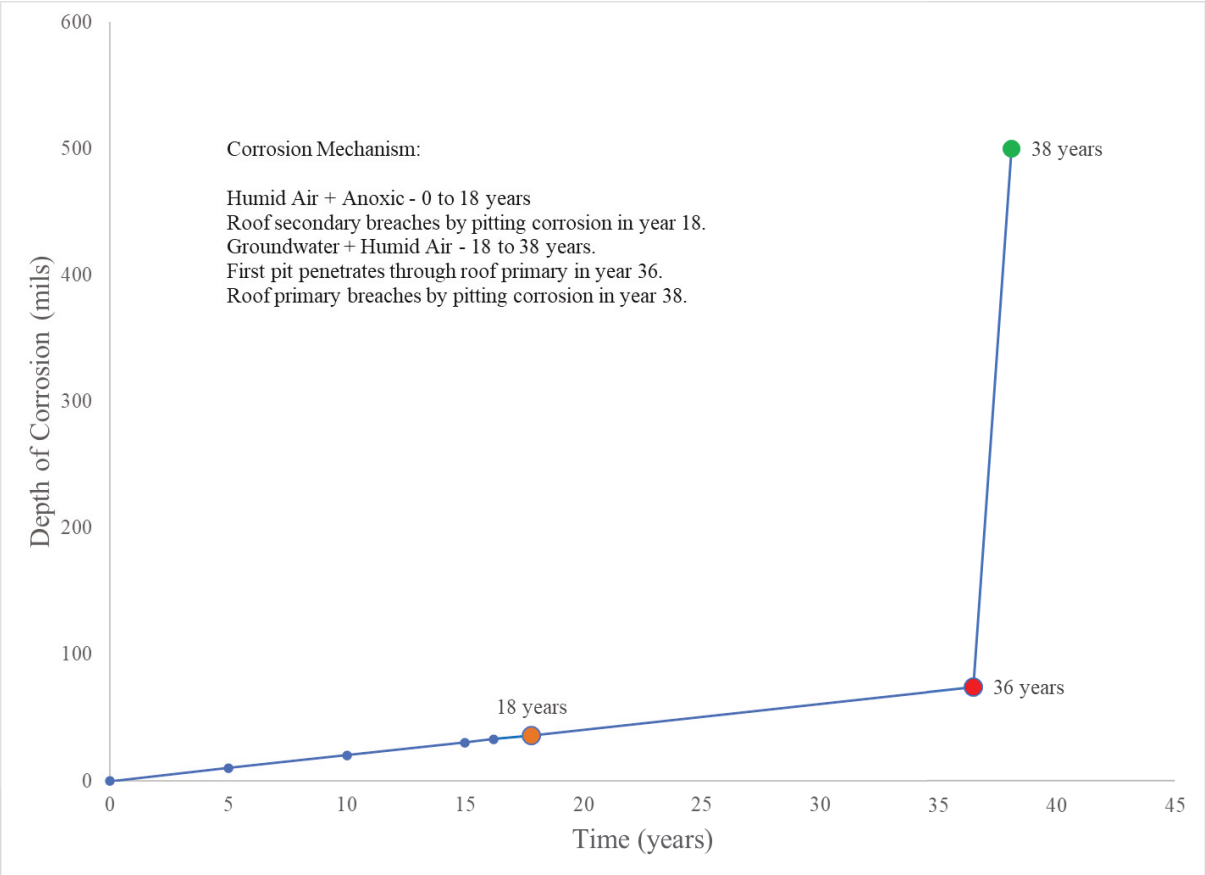

Figure 8-7. Failure of Type III/IIIA Tank for the Saturated Zone, Fast Flow Path Case

Table 8-7. Failure Times for the Saturated Zone, Fast Flow Path Case

		Time (yrs)	Mechanism
Type I Tanks	Roof Primary	23	Groundwater/Humid Air
	Sidewall Secondary	26	Anoxic/Groundwater
	Sidewall Primary	13	Groundwater
	Floor Primary	39	Anoxic/Groundwater
	Floor Secondary	65	Anoxic/Groundwater
	Cooling Coils	38	Humid Air
Type II Tanks	Roof Primary	23	Groundwater/Humid Air
	Sidewall Secondary	26	Anoxic/Groundwater
	Sidewall Primary (Top Knuckle/Top Plate)	14	Groundwater
	Sidewall Primary (Mid Plate)	16	Groundwater
	Sidewall Primary (Bottom Knuckle)	22	Groundwater
	Floor Primary	39	Anoxic/Groundwater
	Floor Secondary	65	Anoxic/Groundwater
	Cooling Coils	38	Humid Air
Type	Roof Secondary	18	Groundwater/Humid Air
	Roof Primary	38	Groundwater/Humid Air
	Sidewall Secondary	20	Anoxic/Groundwater
	Sidewall Primary (Top Knuckle/Top Plate)	13	Groundwater
	Sidewall Primary (Mid Plate)	16	Groundwater
	Sidewall Primary (Bottom Knuckle Type IIIA)	22	Groundwater
	Sidewall Primary (Bottom Knuckle Type III)	19	Groundwater
	Floor Primary	39	Anoxic/Groundwater
	Floor Secondary	59	Anoxic/Groundwater
	Cooling Coils	38	Humid Air
Type IV Tanks	Sidewall	20	Anoxic/Groundwater
	Bottom Knuckle	42	Anoxic/Groundwater
	Floor	39	Anoxic/Groundwater

8.4.2 Vadose Zone

This calculation shows the effect of direct exposure of the steel plates to a corrosive humid air environment. The results are summarized in Table 8-8. The concrete and grout provide essentially no protection, except that initially it was assumed that there was no grout shrinkage next to the floors. Thus, anoxic, passive corrosion could occur in these areas. Humid air results in a general corrosion mechanism and is not as aggressive as the groundwater. Once humid air corrosion commenced, the failure times were typically within 100-200 years.

For this case, it was assumed that both the interior and exterior of the cooling coils were not adequately grouted and that the concrete had degraded. Thus, humid air corrosion occurred on both sides of the pipe wall. Given that the wall thickness for all the cooling coils is 0.154 inches (2 inch, Schedule 40 pipe), the estimated life of the cooling coils before they are penetrated is 38 years (Table 8-8).

Table 8-8. Failure Times for the Vadose Zone, Fast Flow Path Case

		Time (yrs)	Mechanism
Type I Tanks	Roof Primary	123	Humid Air
	Sidewall Secondary	242	Anoxic/Humid Air
	Sidewall Primary	123	Humid Air
	Floor Primary	271	Anoxic/Humid Air
	Floor Secondary	502	Anoxic/Humid Air
	Cooling Coils	38	Humid Air
Type II Tanks	Roof Primary	123	Humid Air
	Sidewall Secondary	242	Anoxic/Humid Air
	Sidewall Primary (Top Knuckle/Top Plate)	139	Humid Air
	Sidewall Primary (Mid Plate)	154	Humid Air
	Sidewall Primary (Bottom Knuckle)	216	Humid Air
	Floor Primary	271	Anoxic/Humid Air
	Floor Secondary	502	Anoxic/Humid Air
	Cooling Coils	38	Humid Air
Type III/IIIA Tanks	Roof Secondary	92	Humid Air
	Roof Primary	123	Humid Air
	Sidewall Secondary	181	Anoxic/Humid Air
	Sidewall Primary (Top Knuckle/Top Plate)	123	Humid Air
	Sidewall Primary (Mid Plate)	154	Humid Air
	Sidewall Primary (Bottom Knuckle Type IIIA)	216	Humid Air
	Sidewall Primary (Bottom Knuckle Type III)	185	Humid Air
	Floor Primary	271	Anoxic/Humid Air
	Floor Secondary	441	Anoxic/Humid Air
	Cooling Coils	38	Humid Air
Type IV Tanks	Sidewall	181	Anoxic/humid air
	Bottom Knuckle	211	Anoxic/humid air
	Floor	226	Anoxic/humid air

9.0 Conclusions

SRS is proceeding with closure of the H-Area Tank Farm (HTF) and F-Area Tank Farm (FTF). Closure consists of removing the bulk waste, heel removal, and filling the tank with tailored grout formulations. This analysis provided an update to the previous PA inputs for steel corrosion.

The Central Scenario for the PA analysis includes three postulated cases: 1) Realistic Case, 2) Compliance Case, and 3) Pessimistic Case. This analysis also included a Fast Flow Path Case. This latter case considered the circumstance where the initial condition of the concrete was in a completely degraded state and that grout shrinkage exposed the steel to the soil environment. In effect, the steel was unprotected by the concrete and grout. The cases have various degrees of conservatism considered. Chemical, physical and tank configuration parameters were investigated to understand their effects on the predicted time to release of the contaminants. The assessment reviewed the initial tank and steel configuration, service life degradation of the steel, and potential corrosion mechanisms associated with degradation of the concrete materials.

The key observations and results from this study follow.

- The progressive degradation model for the steel provides a new approach for the steel corrosion PA input.
- Corrosion mechanism inputs were the same or slightly revised from the previous analysis inputs.
- There is a strong link between the degradation of the concrete and steel corrosion rate. Likewise, there is a link between the steel corrosion and the degradation of the concrete. This steel liner progression model coupled two degradation models to provide SRR with an estimate for the release time of radioactive contaminants to the environment.
- Table 9-1 and Table 9-2 summarize the range of failure times for the various steel components within tanks for each modeling case as a function of waste tank Type.
- Table 9-3 shows the failure times for the cooling coils that are embedded in grout on the interior of the Type I, II, and III/IIIA tanks. The failure time is shown as a function of the assumed case. Given that the pipe is the same size in all the tanks, the failure time is independent of the tank type.
- The models make simple assumptions regarding the corrosion response to a change in the environment and the effects of cracks on the corrosion rate. These assumptions could be refined further to reduce uncertainty in the predicted times.

Table 9-1. Summary of Failure Times (years) for the Saturated Zone for the Scenario Cases by Tank Type

	Saturated Zone			
Tank Type	Realistic Case (years)	Compliance Case (years)	Pessimistic Case (years)	Fast Flow Path Case (years)
I	3929-6250	3929-6250	625-3941	13-65
II	6250-10938	6250-10938	704-6250	14-65
III/IIIA	4688-10938	4688-10938	625-6250	13-59
IV	2495-5469	2495-5469	852-2477	20-42

Table 9-2. Summary of Failure Times (years) for the Vadose Zone for the Scenario Cases by Tank Type

	Vadose Zone			
Tank Type	Realistic Case (years)	Compliance Case (years)	Pessimistic Case (years)	Fast Flow Path Case (years)
I	4008-6250	2960-6250	625-850	123-502
II	6250-10938	4280-8719	704-1136	123-502
III/IIIA	4688-10938	3860-7751	625-1078	92-441
IV	2569-5469	1082-1127	263-367	181-226

Table 9-3. Summary of Cooling Coil Failure Times (years) for Each Scenario Case

Case	**Failure Time (years)**
Realistic Case	1925
Compliance Case	350
Pessimistic Case	350
Fast Flow Path Case	38

10.0 References

[1] Savannah River Remediation, LLC, "Performance Assessment for the F-Tank Farm at the Savannah River Site," SRS-REG-2007-00002, Savannah River Remediation, Aiken, SC, March 2010.

[2] Savannah River Remediation, LLC, "Performance Assessment for the H-Area Tank Farm at the Savannah River Site," SRR-CWDA-2010-00128, Rev. 1, Savannah River Remediation, Aiken, SC, November 2012.

[3] M. E. Denham, "Evolution of Chemical Conditions and Estimated Solubility Controls on Radionuclides in the Residual Waste Layer During Post-Closure Aging of High-Level Waste Tanks," SRNL-STI-2012-00404, Savannah River National Laboratory, Aiken, SC, August 2012.

[4] C. A. Langton, "Chemical Degradation Assessment of Cementitious Materials for the HLW Tank Closure Project," WSRC-STI-2007-00607, Savannah River National Laboratory, Aiken, SC, September 2007.

[5] C. A. Langton, "Chemical Degradation Assessment for the H-Area Tank Farm Concrete Tanks and Fill Grouts," SRNL-STI-2010-00035, Savannah River National Laboratory, Aiken, SC, January 2010.

[6] K. H. Subramanian, "Life Estimation of High Level Waste Tank Steel for F-Tank Farm Closure Performance Assessment," WSRC-STI-2007-00061, Rev. 2, Savannah River National Laboratory, Aiken, SC, June 2008.

[7] B. L. Garcia-Diaz, "Life Estimation of High Level Waste Tank Steel for H-Tank Farm Closure Performance Assessment," SRNL-STI-2010-00047, Savannah River National Laboratory, Aiken, SC, March 2010.

[8] Savannah River Remediation, "Steel Liner Progression Model," G-TTR-H-00017, Savannah River Remediation, Aiken, SC, September 2020.

[9] B. J. Wiersma, "Task Technical and Quality Assurance Plan for Waste Tank Steel Life Progression Model," SRNL-RP-2020-00710, Savannah River National Laboratory, Aiken, SC, October 2020.

[10] G. Flach, "Chemical and Physical Evolution of Tank Closure Cementitious Materials," SRR-CWDA-2021-00034, Savannah River Remediation, Aiken, SC, 2021.

[11] ASTM International, "ASTM A285 / A285M-17, Standard Specification for Pressure Vessel Plates, Carbon Steel, Low- and Intermediate-Tensile Strength," ASTM International, West Conshohocken, PA, 2017.

[12] B. J. Wiersma, "An Investigation of the Potential for Corrosion of the Concrete Rebar in the SRS Waste Tanks," WSRC-TR-93-185, Westinghouse Savannah River Company, Aiken, SC, March 1993.

[13] ASTM International, "ASTM A510/A510M-20, Standard Specification for General Requirements for Wire Rods and Coarse Round Wire, Carbon Steel, and Alloy Steel," ASTM International, West Conshohocken, PA, 2020.

[14] ASTM International, "ASTM A615 / A615M-20, Standard Specification for Deformed and Plain Carbon-Steel Bars for Concrete Reinforcement," ASTM International, West Conshohocken, PA, 2020.

[15] Savannah River Site Drawings, "Type I Waste Tank Concrete Drawings," Savannah River Site, Aiken, SC, 2021.

[16] Savannah River Site Drawings, "Type II Waste Tank Concrete Drawings," Savannah River Site, Aiken, SC, 2021.

[17] B. J. Wiersma, "SRS High Level Waste Tank and Piping Systems - Structural Integrity Program and Topical Report," WSRC-TR-95-0076, Westinghouse Savannah River Company, Aiken, SC, 1995.

[18] ASTM International, "ASTM A516 / A516M-17, Standard Specification for Pressure Vessel Plates, Carbon Steel, for Moderate- and Lower-Temperature Service," ASTM International, West Conshohocken, PA, 2017.

[19] ASTM International, "ASTM A537 / A537M-20, Standard Specification for Pressure Vessel Plates, Heat-Treated, Carbon-Manganese-Silicon Steel," ASTM International, West Conshohocken, PA, 2020.

[20] Savannah River Site, "Type III/IIIA Waste Tank Concrete Drawings," Savannah River Site, Aiken, SC, 2021.

[21] B. J. Wiersma, "An Assessment of the Service History and Corrosion Susceptibility of Type IV Waste Tanks," SRNS-STI-2008-00096, Savannah River National Laboratory, Aiken, SC, September 2008.

[22] Savannah River Site, "Type IV Waste Tank Concrete Drawings," Savannah River Site, Aiken, SC, 2021.

[23] R. S. Waltz, "Annual Radioactive Waste Tank Inspection Program - 2011," SRR-STI-2012-00346, Savannah River Remediation, Aiken, SC, June 2012.

[24] T. L. Davis, "History of Waste Tank 15: 1959 to 1974," DPSPU 77-11-26, E.I. DuPont, Aiken, SC, 1978.

[25] B. J. Wiersma, "In-Service Inspection Program for High Level Waste Tanks," C-ESR-G-00006, Rev. 4 Savannah River National Laboratory, Aiken, SC, March 2014.

[26] B. J. Wiersma, "The Performance of Underground Radioactive Waste Storage Tanks at the Savannah River Site: A 60-year Historical Perspective," *JOM,* vol. 66, no. 3, pp. 471-490, 2014.

[27] J. B. Elder, "Tank Inspection NDE Results for Tank 6 Including Summary of Waste Removal Support in Tanks 5 and 6," SRNL-STI-2009-00560, Savannah River National Laboratory, Aiken, SC, 2010.

[28] B. J. Wiersma, "Analysis of Wall Thinning for Tank 12 During Bulk Oxalic Acid Chemical Cleaning," SRNL-STI-2016-00201, Savannah River National Laboratory, Aiken, SC, 2016.

[29] J. B. Elder, "Tank Inspection NDE Results for Fiscal Year 2019, Waste Tanks 25, 26, 33, 34, 41 & 50," SRNL-STI-2019-00519, Savannah River National Laboratory, Aiken, SC, 2019.

[30] J. B. Elder, "Tank Inspection NDE Results for Fiscal Year 2016, Waste Tanks 39, 40 and 41," SRNL-STI-2016-00454, Savannah River National Laboratory, Aiken, SC, 2016.

[31] S. P. Harris, "Statistical Sampling for In-service Inspection of Liquid Waste Tanks at the Savannah River Site," in *ASME PVP, Paper No. PVP2011-57011*, Metals Park, OH, 2011.

[32] B. J. Wiersma, "Estimation of High Level Waste (HLW) Tank Service Life," WSRC-TR-2005-00196, Savannah River Technology Center, Aiken, SC, 2005.

[33] K. B. Martin, "Corrosion Control Program Description Document," WSRC-TR-2002-00327, Savannah River Remediation, Aiken, 2015.

[34] B. J. Wiersma, "A Structural Impact Assessment of Flaws Detected During Ultrasonic Examination of Tank 15," C-ESR-H-00026, Savannah River National Laboratory, Aiken, SC, 2015.

[35] R. S. Waltz, "SRS High Level Waste Tank Crack and Leak Information," C-ESR-G-00003, Savannah River Remediation, Aiken, SC, 2019.

[36] B. J. Wiersma, "Reference Flaw Size for Types I and II Waste Tanks," WSRC-TR-94-041, Westinghouse Savannah River Company, Aiken, SC, 1994.

[37] B. J. Wiersma, "A Visual Assessment of the Concrete Vaults Which Surround Underground Waste Storage Tanks," WSRC-TR-93-761, Westinghouse Savannah River Company, Aiken, SC, 1993.

[38] J. I. Mickalonis, "Corrosion Evaluation of Tank 40 Leak Detection Box," WSRC-TR-99-00200, Westinghouse Savannah River Company, Aiken, SC, 1999.

[39] B. J. Wiersma, "Coupon Immersion Testing in Simulated Hazardous Low-Level Waste," WSRC-TR-91-493, Westinghouse Savannah River Company, Aiken, SC, 1991.

[40] B. Huet, *Electrochimica Acta,* vol. 51, pp. 172-180, 2005.

[41] C. M. Hansson, "Corrosion of Reinforcing Bars in Concrete," *The Masterbuilder,* pp. 106-124, 2012.

[42] R. M. a. L. J. P. Novak, *Cement and Concrete Research,* vol. 31, p. 589, 2001.

[43] C. Andrade, *Journal of Nuclear Materials,* vol. 358, pp. 82-95, 2006.

[44] X. He, "Carbon Steel Corrosion in Simulated Anoxic Concrete Pore Water for Nuclear Waste Disposal Application," *Corrosion,* vol. 73, no. 11, pp. 1381-1392, 2017.

[45] B. J. Wiersma, "Chemistry Envelope for Pitting and Stress Corrosion Cracking Mitigation," SRNL-STI-2019-00217, Savannah River National Laboratory, Aiken, SC, 2019.

[46] H. Q. Tran, "F-Tank Farm Residual Material Chemical Inventory," CBU-PIT-2005-00157, Westinghouse Savannah River Company, Aiken, SC, 2005.

[47] H. Q. Tran, "H Tank Farm Residual Material Chemical Inventory," CBU-PIT-2005-00216, Westinghouse Savannah River Company, Aiken, SC, 2005.

[48] B. Suprenant, "Beware of Structural Designs that Use Reinforcing Steel for Shrinkage and Temperature Crack Control," *The Voice Newsletter,* June 2016.

[49] L. Bertolini, "Carbonation-Induced Corrosion," in *Corrosion of Steel in Concrete*, Verlag, Wiley VCH, 2004, pp. 79-90.

[50] V. Carevic, "Influence of loading cracks on the carbonation resistance of RC elements," *Construction and Building Materials,* vol. 227, pp. 1-12, 2019.

[51] P. Marques, "Carbonation service life modelling of RC structures for concrete with Portland and blended cements," *Cement and Concrete Composites,* vol. 37, pp. 171-184, 2013.

[52] L. Bertolini, "Chloride-Induced Corrosion," in *Corrosion of Steel in Concrete*, Verlag, Wiley VCH, 2004.

[53] B. J. Wiersma, "Investigation of the Corrosion Behavior of Cooling Coil Material in a Simulated Concrete Environment," WSRC-TR-93-078, Westinghouse Savannah River Company, Aiken, SC, 1993.

[54] U. Angst, "Critical chloride content in reinforced concrete - A review," *Cement and Concrete Research,* vol. 39, pp. 1122-1138, 2009.

[55] D. A. Hausmann, "Steel corrosion in concrete. How does it occur?," *Materials Protection,* vol. 6, pp. 19-23, 1967.

[56] B. J. Wiersma, "Corrosion on the Interior of a Sealed Primary Containment Vessel (PCV) for Research Reactor Fuel," SRNL-L3310-2020-00018, Savannah River National Laboratory, Aiken, SC, 2020.

[57] J. Gonzalez-Sanchez, "Indoor atmospheric corrosion of carbon steel and copper in tropical humid climate," in *Environmental Degradation of Infrastructure and Cultural Heritage in Coastal Tropical Climate*, 2009, pp. 35-51.

[58] J. S. Song, Waste Management, Vol. 9, p. 211-218, 2005.

[59] M. Romanoff, Underground Corrosion, Washington, D.C.: National Bureau of Standards, 1957.

[60] T. M. Sullivan, "Assessment of Release Rates for Radionuclides in Activated Concrete," BNL-71537, Brookhaven National Laboratory, 2003.

[61] K. H. Subramanian, "Corrosion Analysis for Tritium Extraction Facility Disposal in Pre-Disposal Configuration," WSRC-TR-2005-00220, Westinghouse Savannah River Company, Aiken, SC, 2005.

[62] K. H. Logan, *Journal of Research of the National Bureau of Standards,* vol. 22, 1989.

[63] B. Lothenbach, "Cemdata18: A chemical thermodynamic database for hydrated Portland cements and alkali-activated materials," *Cement and Concrete Research,* vol. 115, pp. 472-506, 2019.

[64] E. Giffaut, "Andra thermodynamic database for performance assessment: ThermoChimie," *Applied Geochemistry,* 2014.

[65] F. Uddin, "Effect of Cracking on Corrosion of Steel in Concrete," *International Journal of Concrete Structures and Materials,* 2018.

[66] B. Gerard, "Influence of cracking on the diffusional properties of cement based materials. Part I: Influence of continuous cracks on the steady state regime," *Cement and Concrete Research,* vol. 30, pp. 37-43, 2000.

[67] H. Cho, "Estimation of Concrete Carbonation Depth Considering Multiple Influencing Factors on the Deterioration of Durability for Reinforced Concrete Structures," *Advances in Materials Science and Engineering,* vol. 2016, p. 18, 2016.

[68] B. J. Wiersma, "Service Life Assessment for Repaired Transfer Line Jacket," SRNL-L4400-2014-00015, Rev. 3, Savannah River National Laboratory, Aiken, SC, 2015.

Distribution:

alex.cozzi@srnl.doe.gov
samuel.fink@srnl.doe.gov
connie.herman@srnl.doe.gov
Joseph.Manna@srnl.doe.gov
Gregg.Morgan@srnl.doe.gov
frank.pennebaker@srnl.doe.gov
Boyd.Wiedenman@srnl.doe.gov
Brady.Lee@srnl.doe.gov
Brenda.Garcia-Diaz@srnl.doe.gov
Eric.Skidmore@srnl.doe.gov
Dennis.Jackson@srnl.doe.gov
Cj.bannochie@srnl.doe.gov
Jocelyn.Lampert@srnl.doe.gov
Xiankui.zhu@srnl.doe.gov
Vijay.Jain@srs.gov
kent.rosenberger@srs.gov
steven.thomas@srs.gov
Gregory.flach@srs.gov
Mark.layton@srs.gov
Tim.coffield@srs.gov
Larry.romanowski@srs.gov

Records Administration (EDWS)